

Air Force Institute of Technology

AFIT Scholar

Theses and Dissertations

Student Graduate Works

12-1996

Mass Transport of Volatile Organic Compounds between the Saturated and Vadose Zones

Monte S. Harner

Follow this and additional works at: <https://scholar.afit.edu/etd>



Part of the [Environmental Chemistry Commons](#), and the [Environmental Monitoring Commons](#)

Recommended Citation

Harner, Monte S., "Mass Transport of Volatile Organic Compounds between the Saturated and Vadose Zones" (1996). *Theses and Dissertations*. 5900.

<https://scholar.afit.edu/etd/5900>

This Thesis is brought to you for free and open access by the Student Graduate Works at AFIT Scholar. It has been accepted for inclusion in Theses and Dissertations by an authorized administrator of AFIT Scholar. For more information, please contact AFIT.ENWL.Repository@us.af.mil.

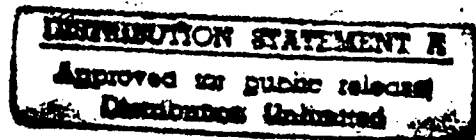


MASS TRANSPORT OF VOLATILE
ORGANIC COMPOUNDS BETWEEN THE
SATURATED AND VADOSE ZONES

THESIS

Monte S. Harner, Captain, USAF

AFIT/GEE/ENV/96D-05



DEPARTMENT OF THE AIR FORCE
AIR UNIVERSITY

AIR FORCE INSTITUTE OF TECHNOLOGY

Wright-Patterson Air Force Base, Ohio

DTIC QUALITY INSPECTED 1

19970214 002

AFIT/GEE/ENV/96D-05

MASS TRANSPORT OF VOLATILE
ORGANIC COMPOUNDS BETWEEN THE
SATURATED AND VADOSE ZONES

THESIS

Monte S. Harner, Captain, USAF

AFIT/GEE/ENV/96D-05

Approved for public release; distribution unlimited

Disclaimer

The views expressed in this thesis are those of the author and do not reflect the official policy or position of the Department of Defense or the U. S. Government.

MASS TRANSPORT OF VOLATILE ORGANIC COMPOUNDS
BETWEEN THE SATURATED AND VADOSE ZONES

THESIS

Presented to the Faculty of the Graduate School of Engineering

Air Education and Training Command

In Partial Fulfillment of the Requirements for the Degree of

Master of Science

in Engineering and Environmental Management

Monte S. Harner, B. S.

Captain, USAF

December 1996

Approved for public release; distribution unlimited

MASS TRANSPORT OF VOLATILE ORGANIC COMPOUNDS
BETWEEN THE SATURATED AND VADOSE ZONES

Monte S. Harner, M.S.
Captain, USAF

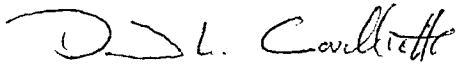
Approved:



Edward C. Heyse, Maj, USAF, BSC
Committee Co-Chairman

25 Nov 96

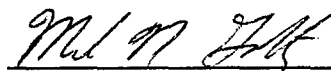
Date



David L. Coulliette, LtCol, USAF
Committee Co-Chairman

25 Nov 96

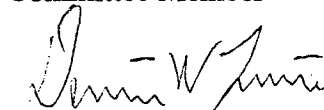
Date



Mark N. Goltz, Ph.D.
Committee Member

25 Nov 96

Date



Dennis W. Quinn, Ph. D.
Committee Member

25 NOV 96

Date

Acknowledgments

I am deeply indebted to my thesis advisor, Major Edward C. Heyse, whose expert advice guided me through the entire thesis process. His insight and direction kept me focused on my research objectives and helped me surmount the many obstacles I encountered. I am also grateful to Lt Col David L. Coulliette and Dr. Dennis W. Quinn for their mathematical expertise. Lt Col Coulliette's knowledge of numerical methods proved indispensable in overcoming the frequent instabilities that plagued my earlier models. The analytical solution, developed by Dr. Quinn, provided a necessary means to validate model results. I am additionally thankful to Dr. Mark N. Goltz for reviewing the preliminary draft of this thesis. His extensive comments and recommendations were instrumental toward the development of a clear and informative final product.

I owe a special gratitude to my wife, Erica, and children, Katelinne and Christopher, for their continual support and understanding throughout this lengthy endeavor. There were countless times when family activities were sacrificed for AFIT obligations. Despite the neglect, they consistently provided the encouragement and motivation I needed to complete the program.

Monte S. Harner

Table of Contents

	Page
Acknowledgments	iii
List of Figures	vi
List of Tables	vii
Abstract	viii
I. Introduction	1
Background	1
Motivation for Research	3
Research Objectives	5
Thesis Overview	5
II. Literature Review	7
Overview	7
Diffusive and Dispersive Transport	7
Advective Transport	9
Partitioning	9
Related Work	10
Conclusion	11
III. Methodology	12
Overview	12
Model Parameters	12
Soil Water Profile Development	15
Contaminant Transport Model Development	17
Model Validation	20
IV. Findings and Analysis.	22
Overview	22
Effect of Soil Type	24
Effect of Infiltration Rate	27

	Page
Effect of Vadose Zone Depth	28
Mass Fraction Returned to Saturated Zone	29
Effect of Model Boundary Conditions	33
 VI. Conclusions	 36
Summary of Significant Findings	36
Recommendations for Future Research	37
 Appendix A: Notation	 38
Appendix B: Soil Water Content Profiles	39
Appendix C: Initial Vadose Zone Concentration Profiles	46
Appendix D: Effect of Soil Type on Contaminant Fate	51
Appendix E: Effect of Infiltration Rate on Saturated Zone Recontamination.	55
Appendix F: Effect of Vadose Zone Depth on Saturated Zone Recontamination	56
Appendix G: Mass Fraction Returned to the Saturated Zone	58
Appendix H: Results Using Gradient Boundary Conditions.	62
Appendix I: Equation Development for Soil Water Content Model	64
Appendix J: Equation Development for Contaminant Transport Model	66
Appendix K: Analytical Solution to Simplified Contaminant Transport Equation	70
Appendix L: FORTRAN computer code for Soil Water Content Model	74
Appendix M: FORTRAN computer code for Contaminant Transport Model	77
References	82
Vita	86

List of Figures

Figure	Page
1. Contamination of Vadose Zone from Saturated Zone	2
2. Recontamination of Saturated Zone from Vadose Zone	3
3. Soil Type Profiles	13
4. Comparison of Model Results with Analytical Solution	21
5. Effect of Soil Type on Contaminant Fate	25
6. Initial Concentration Profile for a Clay Lens Scenario	26
7. Effect of Infiltration Rate on Mass Returned to the Saturated Zone	28
8. Effect of Vadose Zone Depth on Mass Returned to the Saturated Zone	29
9. Mass Fraction Returned to Saturated Zone	31
10. Effect of Boundary Conditions on Flux Across Water Table	35

List of Tables

Table	Page
1. Model Input Parameters	14
2. Model Results--Homogeneous Soil Scenarios	23
3. Model Results--Heterogeneous Soil Scenarios	24
4. Initial Mass Present in Saturated Zone	30
5. Final Results for All Scenarios	32
6. Effect of Boundary Conditions on Mass Fraction Returned	34

Abstract

Volatile organic compounds (VOCs) dissolved in the saturated zone are transported into the vadose zone primarily by gaseous phase diffusion. If the saturated zone is remediated, VOCs present in the vadose zone may become a secondary source of contamination for the groundwater. The amount of VOCs that remain in the vadose zone is dependent on site hydrology, soil properties, and the chemical properties of the contaminants.

The purpose of this study was to determine what conditions caused VOC concentrations in the vadose zone to significantly recontaminate the saturated zone. A one-dimensional numerical model was developed to investigate the transport of a VOC, trichloroethylene, between the saturated and vadose zones under a variety of conditions. The model featured steady-state unsaturated water flow and transient contaminant transport. Transport mechanisms included aqueous phase advection-dispersion and gaseous phase diffusion. Partitioning between the water, gas, and soil compartments were modeled as equilibrium processes. Sensitivity analyses were performed on several variables including soil type (homogeneous and heterogeneous profiles), water infiltration rate, and vadose zone depth. Results indicated that recontamination was most significant in the presence of heterogeneous soils, low infiltration rates and deep vadose zones.

MASS TRANSPORT OF VOLATILE ORGANIC COMPOUNDS BETWEEN THE SATURATED AND VADOSE ZONES

I. Introduction

Background

Roughly half of the U. S. population relies on groundwater as their primary source of drinking water (Tietenberg, 1994). As a result, groundwater contamination by organic compounds has become a major environmental concern. Some primary sources of contamination include: seepage from unlined lagoons and other surface impoundments; leakage from pipes, storage tanks, and equipment; improper disposal practices; and accidental spills (Dragun et al., 1984).

Many of these groundwater contaminants are volatile organic compounds (VOC). In the saturated zone, the transport of dissolved VOCs is normally dominated by aqueous phase advection and dispersion. However, since VOCs have a great tendency to partition into the gaseous phase, they are readily transported into the vadose (or unsaturated) zone (see Figure 1). Once in the vadose zone, VOC transport is predominantly controlled by gaseous phase diffusion (assuming that aqueous phase advection is insignificant as a transport mechanism).

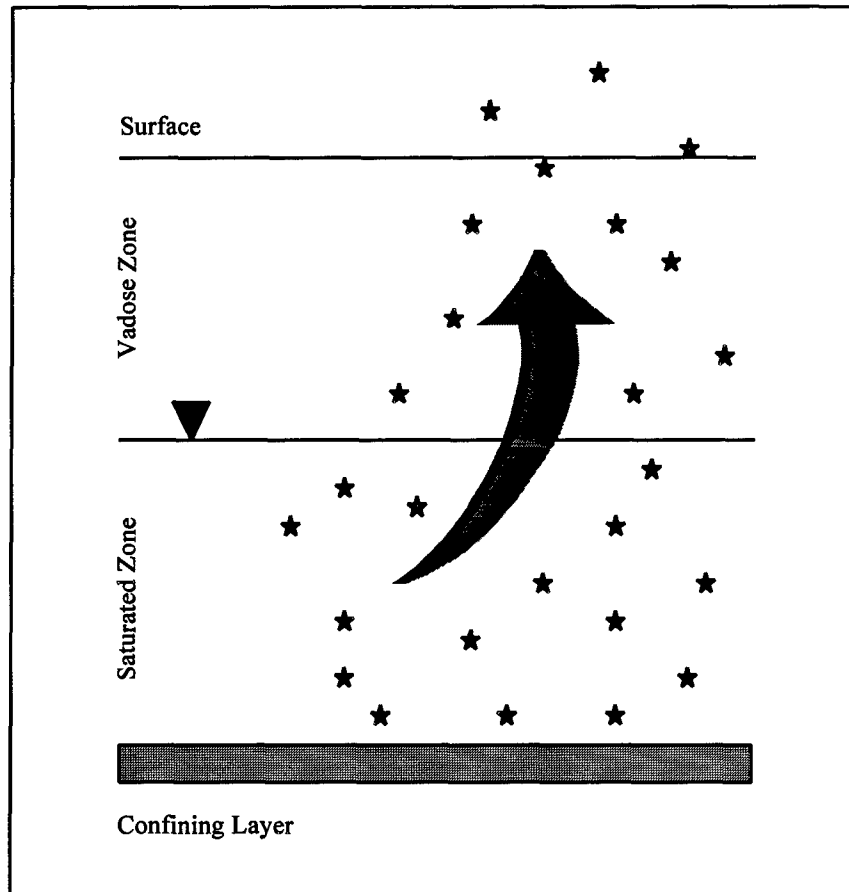


Figure 1. Contamination of Vadose Zone from Saturated Zone

If the groundwater is remediated and VOC concentrations in the saturated zone fall below those in the vadose zone, the resulting concentration gradient will cause VOCs to be transported back into the saturated zone (see Figure 2). Consequently, VOC mass in the vadose zone will become a secondary source of contamination for the saturated zone. The likelihood that such groundwater recontamination would be significant depends upon a myriad of factors, including: site hydrology, soil properties, and the physical and chemical properties of the contaminants themselves.

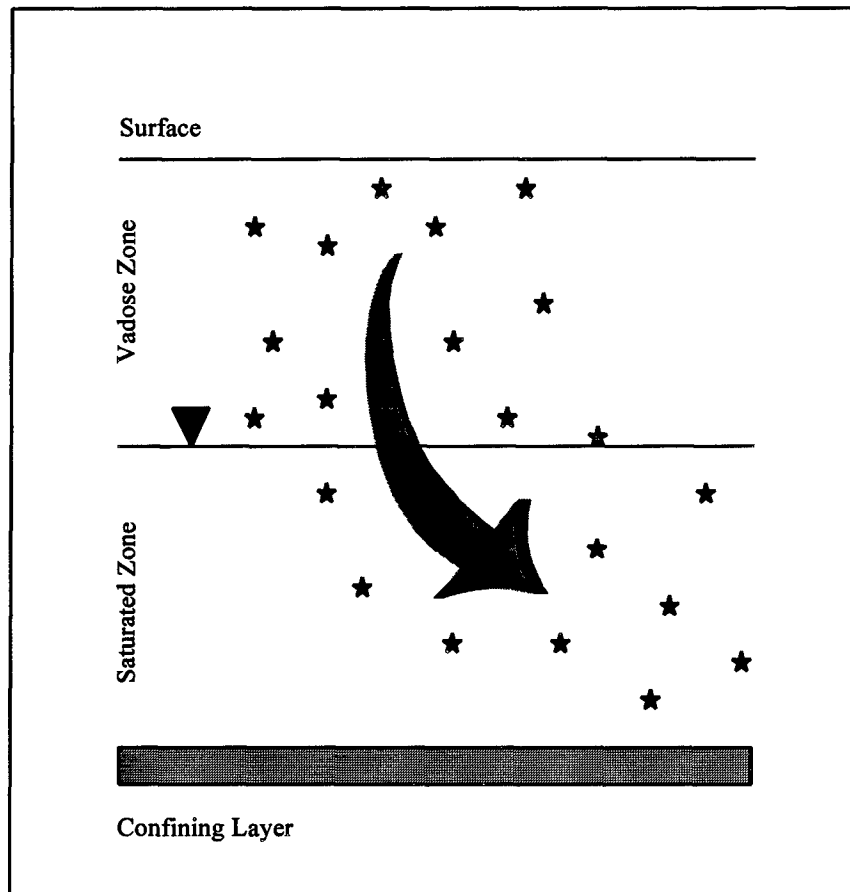


Figure 2. Recontamination of Saturated Zone from Vadose Zone

Motivation for Research

Trichloroethylene (TCE) and other chlorinated organic solvents are some of the most prevalent organic contaminants in U. S. groundwater supplies (Dyksen and Hess, 1982; Conant et al., 1996). Kerfoot and Marrin (1988) reported that TCE, a suspected carcinogen, is the most frequently identified substance at 546 Superfund sites. One Superfund site with widespread TCE contamination is McClellan Air Force Base (AFB), California.

Nearly one-third of McClellan AFB (roughly four square kilometers) is underlain by groundwater that exceeds the maximum contaminant level (MCL) for TCE of 5 µg/L. (Department of the Air Force, 1994). Additionally, the region has experienced changes in the direction of groundwater flow and a decline in the water table since the contamination has occurred. As a result, the base environmental planners maintain that large zones of contamination (principally TCE) have been created in the subsurface both where contaminated groundwater had previously flowed and above where it currently flows. It is important to emphasize that this contamination is unlikely to contain nonaqueous phase liquid (NAPL) free product or ganglia. As far as is known, contamination in these areas was caused solely by the dissolved phase constituents in the groundwater. McClellan's primary concern was that the VOCs that are present in the vadose zone would recontaminate the saturated zone and hinder ongoing groundwater remediation actions. Environmental planners speculated that restoration of these vadose zone areas, in combination with saturated zone remediation, might be necessary.

Currently, the most prevalent vadose zone remediation technology for VOC contamination is soil vapor extraction (SVE) (Merz and Mohr, 1995). However, employing SVE to restore sites of the magnitude of McClellan AFB would be prohibitively expensive. Additionally, the effectiveness of SVE in these situations is uncertain since the fate of the contaminants remains unknown. For example, if a significant fraction of the contaminant mass either escaped into the atmosphere or remained sorbed to the soil matrix, the potential for groundwater recontamination may be

minimal. In such cases, remediation may be unnecessary. Consequently, in order to determine the need for vadose zone restoration, it is important to understand the fate of VOCs in the vadose zone and the conditions under which significant groundwater recontamination may occur.

Research Objectives

- (1) Determine the fate of VOCs which migrate into the vadose zone from the saturated zone.
- (2) Determine the conditions where VOCs in the vadose zone may cause significant recontamination of groundwater.

Thesis Overview

The main body of this thesis is composed of five chapters. Chapter I, "Introduction," provided a brief background on VOC transport between the saturated and vadose zones and justified the focus of this research in the context of an Air Force need. In Chapter II, "Literature Review," the works of other authors are used to identify the predominant contaminant transport mechanisms and validate simplifying assumptions. Chapter III, "Methodology," describes the development and validation of the model utilized in this investigation. It also provides a brief explanation of the parameters selected for sensitivity analysis. Important results are discussed in Chapter IV, "Findings and Analysis." In Chapter V, "Conclusions," the significant findings from this study are summarized and recommendations for future research provided. Additionally, the

attached appendices provide detailed information on notation, model output, equation development, and model computer code.

II. Literature Review

Overview

In the absence of a NAPL phase where density effects and capillary forces may influence contaminant migration (Kerfoot and Marrin, 1988; Falta et al., 1989; Frind and Mendoza, 1990a), the potential transport mechanisms controlling the movement of VOCs between the saturated and vadose zones are limited to aqueous and gaseous phase diffusion, dispersion, and advection; and partitioning between the aqueous, gaseous, and solid phases. The extent to which each of these processes contributes to the mass transfer of VOCs is dependent on both the conditions in the subsurface and the properties of the contaminant.

Diffusive and Dispersive Transport

Diffusion is defined as the process by which a solute moves from an area of higher concentration toward an area of lower concentration. Such transport occurs by both the random thermal motion of molecules (molecular diffusion) and by their interaction with pore walls (Knudsen diffusion). Though Knudsen diffusion has been shown to be significant in packed soil columns by one study (Alzaydi et al., 1978), very little additional research on the topic was attainable. In fact, the explicit evaluation of such diffusion has been generally ignored by soil scientists and hydrologists. Instead, its effect is usually implicitly lumped into the tortuosity factor (Kreamer et al., 1988).

Diffusive transport through the vadose zone occurs in both the aqueous and gaseous phases. However, since diffusion coefficients for VOCs in air may be several orders of magnitude greater than those in water, gaseous diffusion should be the predominant process (Baehr, 1987; Sleep and Sykes, 1989). Several researchers have found gaseous diffusion to be a very significant transport mechanism (Farmer et al., 1980; Earp et al., 1982; Marrin and Thompson, 1987). Nonetheless, aqueous phase diffusion may not always be negligible. In unsaturated soils possessing high water contents (e.g., clays) or in areas near the water table where gas phase porosity is very low, aqueous diffusion may be an important mechanism for VOC transport (Baehr, 1987).

Several authors have also studied the effect of temperature on diffusive transport (Kreamer et al., 1988; Frind and Mendoza, 1990b; Conant et al., 1996). In all these studies, the researchers concluded that the vadose zone temperature variations typically encountered in most climates had relatively insignificant effects on diffusive rates. Thus, it is a reasonable assumption to neglect the influence of temperature on diffusive transport.

Mechanical dispersion refers to the mixing of a solute, as it travels through a porous medium, due to differential pore sizes, differential path lengths, and pore friction (Fetter, 1993). This mechanism is inherently dependent on the advective flux and it may only be neglected when advection is insignificant.

Advective Transport

Advection describes the transport of a contaminant due to the motion of the fluid containing it. As with diffusion, advective transport through the vadose zone may occur in both the aqueous and gaseous phases. In general, aqueous advection is caused by water infiltrating from the surface (McAlary and Mendoza, 1990). Consequently, this transport mechanism is greatly influenced by the hydraulic conductivity of the soil and the precipitation rate at the surface.

Gaseous advection is commonly assumed to be negligible (Faust, 1985; Baehr, 1987; Abriola, 1989). This assumption is usually considered to be reasonable in the absence of a NAPL phase (Abriola and Pinder, 1986). Additionally, Farrier and Massmann (1992) studied the influence that atmospheric pressure variations induced on advective transport in the vadose zone. They found that though barometric pressure may have notable short-term effects, in the long-term, these effects could be considered negligible. Also, others have reported that water table fluctuations have had no discernible effect on advective processes (Earp et al., 1982; Kremer et al., 1988).

Partitioning

Partitioning refers to the process by which a chemical becomes distributed among the separate phases present in the soil matrix. Without a NAPL phase, air/water and soil/water partitioning are usually the dominant mechanisms. Furthermore, several

researchers have shown soil/air partitioning (vapor sorption) to only be significant in very dry soils (Chiou and Shoup, 1985; Lion et al., 1988; Culver et al., 1992).

Additionally, local equilibrium is commonly assumed in the literature (Baehr, 1987; Kremer et al., 1988; Conant et al., 1996). This implies that “within some short time scale (essentially instantaneously) contiguous phases reach a thermodynamic equilibrium. Thus, the mass fraction of a species in one phase can be related to the mass fractions of this same species in the other phases via partition expressions” (Abriola, 1989). The validity of this assumption at the field scale has not been confirmed. However, studies that employ the local equilibrium assumption (LEA) tend to overestimate the extent of contamination (Abriola, 1989), which implies that it is a conservative approach.

Related Work

There is a vast amount of literature that concerns contaminant transport in the vadose zone. However, most of these works focus on the contamination of the saturated zone from a NAPL source in the vadose zone (Baehr, 1987; Falta et al., 1989; Sleep and Sykes, 1989; McAlary and Mendoza, 1990; Frind and Mendoza, 1990a; Conant et al., 1996). Only a minority of authors have studied the volatilization of contaminants into the vadose zone from the saturated zone

In one field study, Barber et al. (1990) investigated the transport of methane from the saturated zone to the vadose zone and found that the process was dominated by

diffusion. Using a simple, steady-state diffusion model, they obtained fair agreement with field data, but the assumption of constant diffusion with depth and the neglect of other processes such as advection and sorption restricts the general applicability of the model.

Johnson and McCarthy (1993) conducted laboratory experiments to study the transport of TCE from groundwater to the vadose zone and also determined that diffusion was the controlling vertical transport mechanism. They found that TCE concentrations decreased several orders of magnitude across the capillary fringe. Numerical models were developed which incorporated variable water contents and diffusion coefficients with depth. Both one- and two-dimensional simulations agreed well with experimental results. Johnson and McCarthy's work, however, was limited to a very shallow homogeneous soil and did not consider vertical water flow.

Conclusion

This research advances our understanding of unsaturated contaminant transport. It extends the work of Johnson and McCarthy (1993) by addressing the impact of soil type (both homogeneous and heterogeneous soil profiles), water infiltration, and vadose zone depth on the transport of VOCs between the saturated and vadose zones. Of primary importance is the potential for VOCs in the vadose zone to recontaminate the saturated zone.

III. Methodology

Overview

The mass transport of the contaminant was estimated using a conservation of mass approach. Variable soil water profiles were approximated by assuming steady-state water flow. This method yielded a partial differential equation which was solved via a finite-difference approximation. The resulting numeric model was then validated against a simplified analytical solution. Sensitivity analyses were conducted on soil type, infiltration rate, and vadose zone depth.

Model Parameters

For this study, five different soil profiles were investigated--three homogeneous and two heterogeneous (see Figure 3). In the homogeneous scenarios, the vadose zone was modeled as a single soil type (*Sand, Loam, or Clay*). These soil types follow the U.S. Department of Agriculture (USDA) textural classifications and the parameter values selected represent mean estimates published by Maidment (1993). All model parameter values are listed in Table 1. Sand, loam, and clay were chosen to provide information across a wide range of soil types. The heterogeneous scenarios included modeling a sandy soil bisected by a 50-cm thick clay lens (*Lens*), and a system with alternating 25-cm layers of sand, loam, and clay (*Layered*). The purpose of the layered case was to

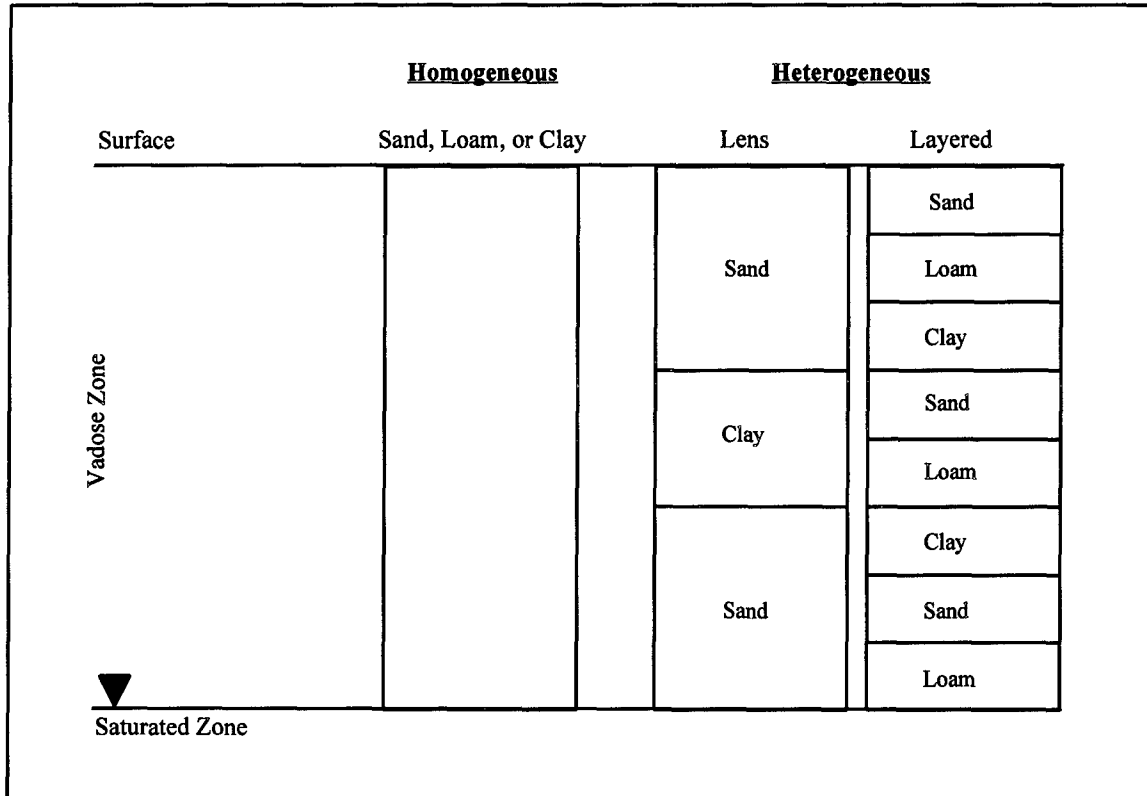


Figure 3. Soil Type Profiles

simulate very heterogeneous conditions. To avoid confusion, the five soil profiles modeled will be categorized as simply *soil types* for the remainder of this paper.

The aqueous phase advective flux was assumed to be constant and dominated by the water infiltrating from the surface. The use of a constant infiltration rate is most reasonable for moderate and thick vadose zones; it may not be appropriate for porous, shallow soils whose water contents are greatly influenced by rainfall events.

Nonetheless, steady state infiltration will be assumed to be adequate for the purpose of this study. The infiltration rates were estimated by assuming that two-thirds of the annual precipitation penetrates into the soil (T. Steenhuis, "Fast Moving Solutes in the Vadose

Table 1: Model Input Parameters

Soil Properties ^a	USDA Soil Classification ^f			
	Sand	Loam	Clay	
Saturated volumetric water content	0.417	0.434	0.385	
Residual volumetric water content	0.020	0.027	0.090	
Saturated hydraulic conductivity [cm/day]	500	30	1	
Effective porosity	0.417	0.434	0.385	
Solids bulk density [g/cm ³]	1.55	1.45	1.35	
Bubbling pressure [cm]	7.26	11.15	37.30	
Pore-size distribution index	0.694	0.252	0.165	
TCE Properties at 20 °C				
Initial aqueous concentration in saturated zone [mg/L]	5.0			
Free water molecular diffusion coefficient [cm ² /day]	0.729 ^b			
Free air molecular diffusion coefficient [cm ² /day]	6993 ^c			
Solids/Water distribution coefficient [cm ³ /g]	0.118 ^d			
Henry's law constant	0.350 ^e			
Other Parameters				
Hydraulic gradient (saturated zone)	0.02			
Vertical aqueous phase advective flux [cm/day] ^f	0.00	0.04	0.20	0.40
Total depth of vadose zone [cm] ^f	300	1000	3000	
Longitudinal dispersivity in vadose zone [cm] ^{a,g}	30	100	300	
Transverse dispersivity in vadose zone [cm] ^h	3	10	30	

^a From Maidment (1993)

^b Estimated by Hayduk and Laudie method (Lyman et al., 1982)

^c Estimated by Fuller, Giddings, and Schettler method (Lyman et al., 1982)

^d Estimated using regression from Chiou et al. (1979)

^e From Howe et al. (1987)

^f Values varied for sensitivity analysis

^g Values estimated using Peclet number of 10

^h Values estimated to be 1/10 of longitudinal dispersivity

Zone." Environmental Hydrology Colloquium, Department of Civil and Environmental Engineering, University of Cincinnati, OH, 23 February 1996). Precipitation rates were selected to depict semi-arid, temperate, and subtropical climates (Maidment, 1993). This provided a reasonable range of infiltration rates for the simulations (see Table 1). The

zero infiltration rate scenario served as a baseline case from which the reliability of the model could be verified. Vadose zone thicknesses vary widely in the field, and the soil depths modeled were chosen to reflect this attribute. The range of values selected span shallow, moderate, and deep soil layers (see Table 1). The VOC selected for this study was TCE.

Soil Water Profile Development

The water content profiles were used to estimate the distribution of water through the entire vadose zone depth. Unfortunately, water content is often discontinuous in space due to varying matrix properties (Abriola, 1989). This makes solving for the water content as a function of depth, directly, very difficult. However, the pressure head, which is always continuous, may be determined more readily.

Buckingham's flux law, shown as Equation (1), describes the flow of water through an unsaturated soil (Buckingham, 1907):

$$q_{wz} = -K(\Psi) \left(\frac{\partial(\Psi)}{\partial z} + 1 \right) \quad (1)$$

(Note: All notation used in this paper are defined in Appendix A.)

The function $K(\Psi)$ in Equation (1) was expressed by the van Genuchten (1980) relationship presented in Equation (2):

$$K(\Psi) = \frac{K_s \left[1 - (\alpha\Psi)^{\beta-1} \left[1 + (\alpha\Psi)^\beta \right]^{-m} \right]^2}{\left[1 + (\alpha\Psi)^\beta \right]^{\frac{m}{2}}} \quad (2)$$

The van Genuchten soil parameters (α , β , and m) in Equation (2) were calculated from the Brooks and Corey parameters (h_b and λ) using the relationships shown in Equations (3), (4), and (5) (Maidment, 1993). The values used for h_b and λ are listed in Table 1:

$$\alpha = (h_b)^{-1} \quad (3)$$

$$\beta = \lambda + 1 \quad (4)$$

$$m = \frac{\lambda}{\lambda + 1} \quad (5)$$

Assuming that the water infiltration rate was constant, a finite-difference approximation of Equation (1) was solved iteratively to determine the pressure head as a function of depth in the vadose zone, ($\Psi(z)$). The solution technique began at the water table where, by definition, the pressure head is zero, and propagated upward to the surface. Once $\Psi(z)$ was determined, the water content profile was calculated using Equation (6) (van Genuchten, 1980):

$$\theta_w(z) = \theta_r + \frac{\theta_s - \theta_r}{\left[1 + [\alpha\Psi(z)]^\beta\right]^m} \quad (6)$$

Soil water content profiles were developed for each soil type, infiltration rate, and soil depth scenario; and are illustrated in Appendix B. Also, Appendix I contains a more detailed description of the equation development used for this model and identifies the assumptions employed. The FORTRAN computer code for the model is listed in Appendix L.

Contaminant Transport Model Development

This model assumes that no NAPL phase exists and that the air phase is immobile (gaseous advection negligible). Additionally, it is assumed that the soil grains are covered with a continuous film of water; therefore, vapor sorption is negligible (Frind and Mendoza, 1990a). Since TCE does not readily degrade aerobically, it is further assumed that all other sources or sinks are insignificant, as well. Consequently, the one-dimensional mass transport equation reduces to Equation (7):

$$\frac{\partial}{\partial t}(\theta_w C_w + \theta_a C_a + \rho_b C_s) = -\frac{\partial}{\partial z}(q_{wz} C_w) + \frac{\partial}{\partial z}\left(D_w \frac{\partial C_w}{\partial z} + D_a \frac{\partial C_a}{\partial z}\right) \quad (7)$$

where:

$$D_w = \left[D_{fw} + \alpha_T \left(\frac{q_{wx}}{\theta_w} \right) + \alpha_L \left(\frac{q_{wz}}{\theta_w} \right) \right] \theta_w \tau_w \quad (8)$$

$$D_a = D_{fa} \theta_a \tau_a \quad (9)$$

$$\theta_a = n - \theta_w \quad (10)$$

$$q_{wx} = K(\theta_w) \frac{\partial h}{\partial x} \quad \left(\frac{\partial h}{\partial x} \text{ is the hydraulic gradient} \right) \quad (11)$$

Note that in Equation (8), D_w incorporates mechanical dispersion from two different sources. The term, $\alpha_T \left(\frac{q_{wx}}{\theta_w} \right)$, simulates the dispersion caused by the vertical movement of water (upward) induced by the horizontal groundwater flow. The parameter, q_{wx} , was calculated using Equation (11) by assuming a constant hydraulic gradient through the saturated zone (the values for θ_w and $K(\theta_w)$ vary with depth and were determined by the

soil water content model). The effect of this dispersion term only is significant near the water table where the soil water content (and hydraulic conductivity) is relatively high.

The other term, $\alpha_L \left(\frac{q_{wz}}{\theta_w} \right)$ represents the dispersion due to the infiltrating water.

The contaminant flux through the porous media is described by Equation (12):

$$J = q_{wz}C_w - D_w \frac{\partial C_w}{\partial z} - D_a \frac{\partial C_a}{\partial z} \quad (12)$$

Assuming local equilibrium and linear partitioning, all sorbed and air concentrations may be written in terms of the aqueous concentration as shown in Equations (13) and (14) respectively:

$$C_s = K_d C_w \quad (13)$$

$$C_a = K_H C_w \quad (14)$$

The Millington method is used to estimate the air and water tortuosities as shown in Equations (15) and (16) respectively (Millington, 1959). This method is commonly employed in the literature (Baehr, 1987; Culver et al., 1991; Conant et al., 1996):

$$\tau_w = \frac{(\theta_w)^{7/3}}{n^2} \quad (15)$$

$$\tau_a = \frac{(\theta_a)^{7/3}}{n^2} \quad (16)$$

Incorporating Equations (13) through (16) into Equation (7) and assuming steady state vertical water flow, the mass transfer equation simplifies to Equation (17):

$$\frac{\partial C_w}{\partial t} = -\left(\frac{q_{wz}}{R_w}\right) \frac{\partial C_w}{\partial z} + \frac{1}{R_w} \frac{\partial}{\partial z} \left[(D_w + D_a K_H) \frac{\partial C_w}{\partial z} \right] \quad (17)$$

where the retardation factor, R_w , is described by Equation (18):

$$R_w = \theta_w + \theta_a K_H + \rho_b K_d \quad (18)$$

Likewise, the contaminant flux in Equation (12), reduces to Equation (19):

$$J = q_{wz} C_w - (D_w + D_a K_H) \frac{\partial C_w}{\partial z} \quad (19)$$

Equation (17) was approximated with finite differences using a Crank-Nicolson method modified to include the advection term. The truncation error of both of these methods is $O(\Delta z)^2$ (order delta-z squared). Equation (19) was also approximated as a finite difference using a backward-difference method with an error $O(\Delta z)$ (Mayers and Morton, 1994). The accuracy of these methods is assumed to be sufficient for the purpose of this research. The finite-difference approximations for Equations (17) and (19) were solved using Dirichlet boundary conditions. The upper boundary (surface) was fixed at a zero concentration. To simulate the initial contamination of the vadose zone, the lower boundary (water table) was set at a constant aqueous concentration of 5 mg/L, which is 1000 times greater than the MCL for TCE, and each scenario was run for 2000 simulated days. The resulting vadose zone concentration profiles (hereinafter referred to as the initial concentration profiles) are illustrated in Appendix C. Then, to simulate the recontamination of the saturated zone, the lower boundary condition was abruptly set to

zero and simulations continued until either the highest aqueous concentration in the vadose zone fell below 1 µg/L (1/5 of the MCL) or another 2000 days was reached. A more detailed equation development for the contaminant transport model is included in Appendix J. Also, the model's FORTRAN computer code is listed in Appendix M.

Model Validation

The numerical model was validated against an analytical solution. If the mass transport equation shown in Equation (17) is simplified by assuming that the advection and diffusion-dispersion terms are constant in space, the equation has the analytical solution described as Equation (20):

$$C_w(z, t) = \frac{C_i}{L}z + e^{\frac{Uz}{2D}} \left(\sum_{k=1}^{\infty} \alpha_k(t) \sin \frac{k\pi z}{L} \right) \quad (20)$$

where:

$$U = \frac{q_{wz}}{\theta_w} \quad (21)$$

$$D = D_w + D_a K_H \quad (22)$$

$$\alpha_k(t) = \alpha_k(0)e^{-\omega_k t} + \frac{\gamma_k}{\omega_k} (1 - e^{-\omega_k t}) \quad (23)$$

$$\alpha_k(0) = \frac{2k\pi C_i}{L^2} \left[\frac{e^{\frac{UL}{2D} \cos(k\pi)}}{\frac{U^2}{4D^2} + \frac{k^2\pi^2}{L^2}} + \frac{\frac{U}{DL} \left(e^{\frac{UL}{2D} \cos(k\pi)} - 1 \right)}{\left(\frac{U^2}{4D^2} + \frac{k^2\pi^2}{L^2} \right)^2} \right] \quad (24)$$

$$\gamma_k = \frac{8k\pi D^2 UC_i}{4k^2\pi^2 D^2 L + U^2 L^3} \left(e^{-\frac{UL}{2D} \cos(k\pi)} - 1 \right) \quad (25)$$

$$\omega_k = \frac{U^2}{4D} + D \frac{k^2\pi^2}{L^2} \quad (26)$$

The complete derivation of Equations (20) through (26) is provided in Appendix K. A comparison between the results of the model and the analytical solution shows that the data are nearly identical (see Figure 4). This outcome provides creditability for the model results. Unfortunately, no suitable field or experimental data was attainable for further verification.

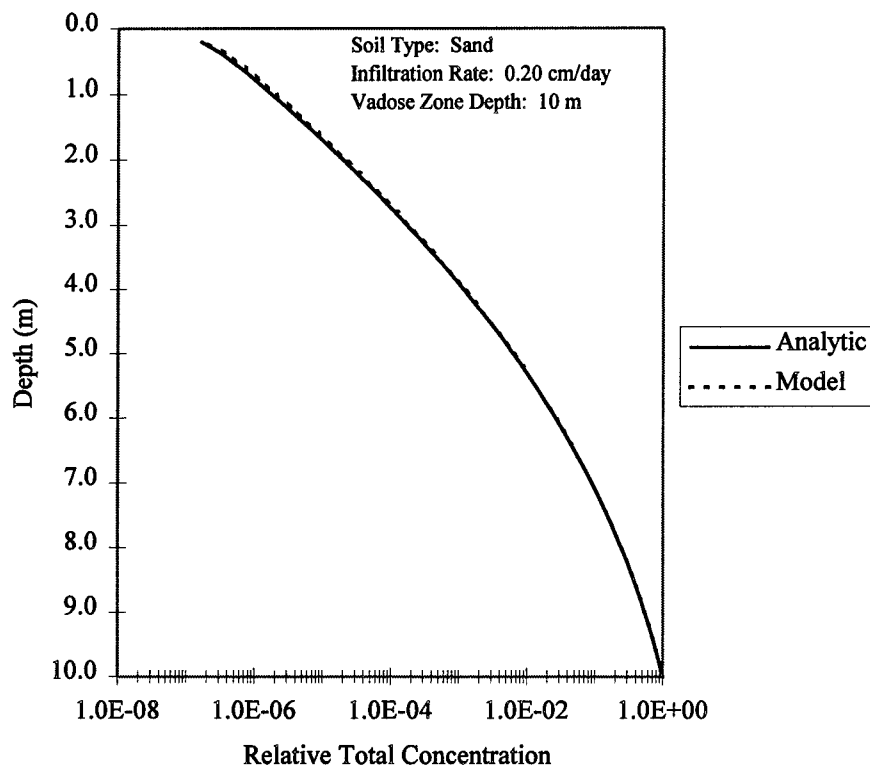


Figure 4: Comparison of Model Results with Analytical Solution

IV. Findings and Analysis

Overview

Sensitivity analyses were conducted by varying soil type (both homogeneous and heterogeneous profiles), water infiltration rate, and vadose zone depth. Mass balance was checked by comparing the initial total mass of contaminant present in the vadose zone to the amount of mass transferred into the atmosphere, plus the amount remaining in the vadose zone, plus the amount transferred back into the saturated zone. The mass present in the vadose zone was calculated by integrating the initial and final concentration profiles over space. The amount transferred into the atmosphere or saturated zone was determined by integrating the respective contaminant flux over time. Results which were within $\pm 10\%$ of the initial mass were considered to be acceptable.

Unfortunately, several scenarios exhibited mass balance problems that could not be overcome. Cases where high infiltration rates were coupled with deep vadose zones proved to be most troublesome. These scenarios experienced very rapid concentration drops which created large errors in the numerical solution technique. The homogeneous clay and heterogeneous lens soil profiles were also difficult to determine. Despite these deficiencies, the quantity of acceptable results was sufficient to observe trends in the data and to develop reasonable conclusions. Tables 2 and 3 list the model results for the homogeneous and heterogeneous scenarios respectively.

Table 2: Model Results--Homogeneous Soil Scenarios

Sand						Loam						
	Infiltration Rate (cm/day)				Depth (m)		Infiltration Rate (cm/day)				Depth (m)	
	0.00	0.04	0.20	0.40			0.00	0.04	0.20	0.40		
M_i	1.09	1.52	1.80	1.80	3	M_i	0.77	1.69	0.69	0.59	3	
M_a	0.70	0.91	0.84	0.61		M_a	0.49	0.47	0.00	0.00		
M_s	0.00	0.00	0.00	0.00		M_s	0.00	0.09	0.00	0.00		
M_w	0.37	0.59	0.93	1.14		M_w	0.26	1.10	0.67	0.58		
% M_i	98	99	98	98		% M_i	98	98	97	99		
M_i	6.40	8.51	7.72	5.71	10	M_i	3.06	3.49	1.82	1.76	10	
M_a	3.24	3.36	1.88	0.57		M_a	1.79	0.01	0.00	0.00		
M_s	0.00	0.00	0.00	0.00		M_s	0.35	0.99	0.01	0.00		
M_w	3.14	5.12	5.74	4.98		M_w	0.78	2.29	1.66	1.64		
% M_i	100	100	99	97		% M_i	95	95	92	94		
M_i	23.58	22.37	-----	7.28	30	M_i	8.63	5.42	-----	-----	30	
M_a	8.30	3.75	-----	0.01		M_a	1.04	0.00	-----	-----		
M_s	0.86	4.11	-----	0.25		M_s	4.43	1.34	-----	-----		
M_w	14.26	14.34	-----	7.39		M_w	2.71	3.53	-----	-----		
% M_i	99	99	-----	105		% M_i	95	90	-----	-----		

Clay						
	Infiltration Rate (cm/day)				Depth (m)	
	0.00	0.04	0.20	0.40		
M_i	0.85	0.69	0.57	E	3	
M_a	0.04	0.00	0.00	E		
M_s	0.34	0.02	0.00	E		
M_w	0.43	0.61	0.54	E		
% M_i	95	91	95	E		

All results for clay with vadose zone depths of 10 and 30 m exhibited significant mass balance errors

Notation:

- result exhibited mass balance errors
- M_i initial mass in vadose zone
- M_a mass transferred to the atmosphere
- M_s mass remaining in vadose zone
- M_w mass transferred to the saturated zone
- % M_i % of M_i accounted for by mass balance

Table 3: Model Results--Heterogeneous Soil Scenarios

Lens						Layered					
	Infiltration Rate (cm/day)				Depth (m)		Infiltration Rate (cm/day)				Depth (m)
	0.00	0.04	0.20	0.40			0.00	0.04	0.20	0.40	
M_i	3.08	3.00	2.73	-----	3	M_i	2.45	2.10	1.27	1.13	3
M_a	0.38	0.09	0.06	-----		M_a	0.65	0.03	0.00	0.00	
M_s	0.00	0.00	0.00	-----		M_s	0.10	0.10	0.00	0.00	
M_w	2.67	2.88	2.73	-----		M_w	1.68	1.94	1.23	1.22	
% M_i	99	99	102	-----		% M_i	99	99	98	108	
M_i	8.67	10.00	-----	-----	10	M_i	3.23	3.62	2.79	2.65	10
M_a	1.81	0.44	-----	-----		M_a	0.28	0.00	0.00	0.00	
M_s	0.00	0.00	-----	-----		M_s	0.97	0.56	0.06	0.03	
M_w	6.83	9.48	-----	-----		M_w	1.92	2.98	2.53	2.49	
% M_i	100	99	-----	-----		% M_i	98	98	93	95	
M_i	24.94	23.15	-----	-----	30	M_i	4.05	5.62	-----	-----	30
M_a	4.39	0.64	-----	-----		M_a	0.00	0.00	-----	-----	
M_s	1.15	4.71	-----	-----		M_s	1.45	1.09	-----	-----	
M_w	18.96	18.66	-----	-----		M_w	2.57	3.99	-----	-----	
% M_i	98	104	-----	-----		% M_i	99	90	-----	-----	

Notation:

----- result exhibited mass balance errors

M_i initial mass in vadose zone

M_a mass transferred to the atmosphere

M_s mass remaining in vadose zone

M_w mass transferred to the saturated zone

% M_i % of M_i accounted for by mass balance

Effect of Soil Type

Model results show that soil type does significantly affect the overall fate of VOCs in the vadose zone, particularly at deeper soil depths. Moreover, it is apparent that in certain instances, heterogeneities in the soil profile may substantially increase the potential for contaminant migration back into the saturated zone. Though each scenario

had somewhat unique results, Figure 5 illustrates one fairly representative case. All other soil type results are summarized in Appendix D.

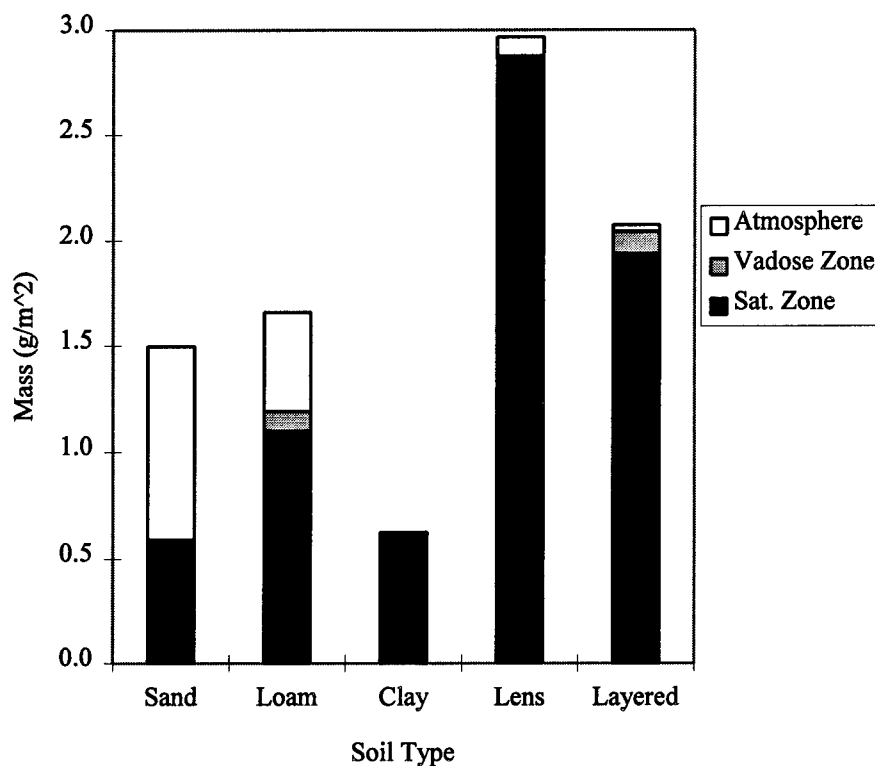


Figure 5: Effect of Soil Type on Contaminant Fate
(Infiltration Rate: 0.04 cm/day; Vadose Zone Depth: 3 m)

Figure 5 indicates that, with the exception of sand, only a small fraction of contaminant mass is lost into the atmosphere and very little, if any, remains in the vadose zone. The majority of the mass is transported back into the saturated zone. On one extreme, thin sandy soils allow rapid transport to the surface and experience relatively large losses to the atmosphere. Conversely, the low conductivity of clayey soil impedes

significant transport of contaminants from the saturated zone to the vadose zone. Thus for both of these cases, little contaminant is available for recontamination of the groundwater.

Figure 5 also shows, however, that soil heterogeneities may create opportunities for substantial recontamination of the saturated zone. In these cases, highly permeable layers (e.g. sand) encourage significant migration up through the vadose zone until a low permeable layer (e.g. clay) is encountered which hinders transport. Thus, below a clay layer, substantial contaminant mass may accumulate (see Figure 6).

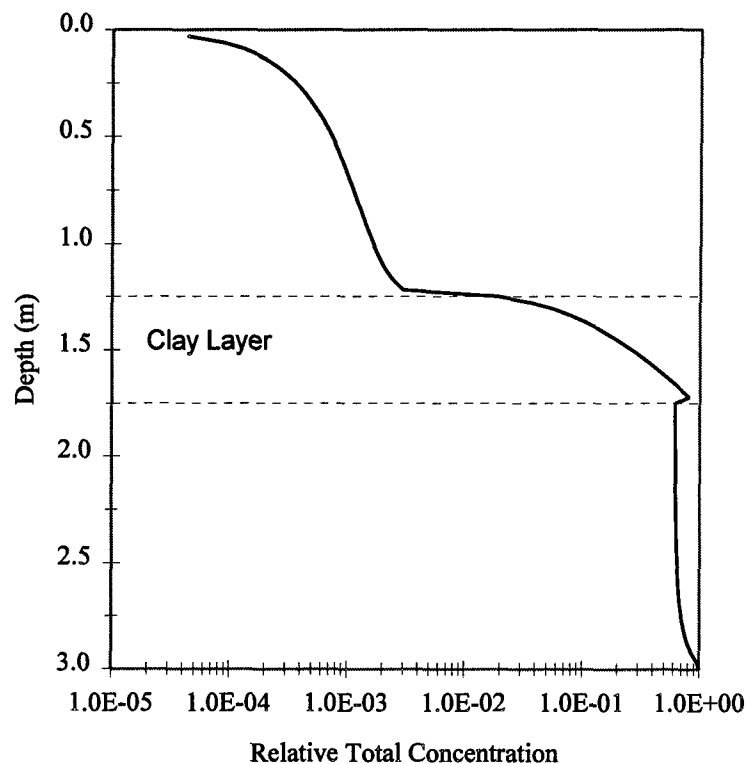


Figure 6: Initial Concentration Profile for a Clay Lens Scenario
(Soil Type: Lens; Infiltration Rate: 0.04 cm/day; Vadose Zone Depth: 3 m)

Figure 6 illustrates the initial contaminant concentration profile for one of the clay lens scenarios. It clearly shows a large amount of mass present immediately below the clay layer. Once the saturated zone is remediated and the concentration gradient is reversed, this large mass will be transferred back into the groundwater potentially causing significant recontamination. Of the two heterogeneous soils modeled, the clay lens scenarios consistently proved to be the worst cases (returned most mass to the saturated zone).

Effect of Infiltration Rate

Water infiltration also seems to have a significant effect on the extent of recontamination. For most soils under normal infiltration rates (between 0.04 and 0.4 cm/day), the mass returned to the saturated zone decreases with increasing infiltration rate (see Figure 7). In these situations, the downward movement of water actually limits contaminant transport up into the vadose zone from the saturated zone. Consequently, since less mass is present in the vadose zone, less significant recontamination of the saturated zone occurs. Only under very low infiltration rates (< 0.04 cm/day) does the water movement become too insignificant to combat the upward diffusion-dispersion contaminant transport. Sand is the exception which shows a continual increase in mass returned with infiltration rate. The high porosity of this soil allowed diffusive-dispersive processes to dominate throughout the range of infiltration rates used in this case. Under other scenarios (i.e. ones using deeper soils), however, the trend where mass returned

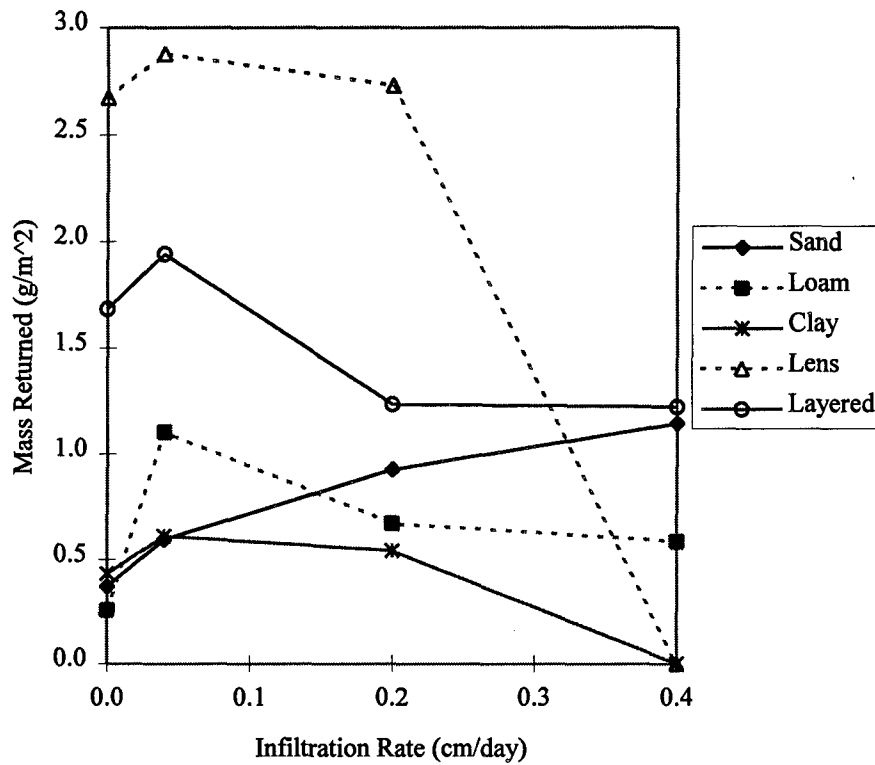


Figure 7: Effect of Infiltration Rate on Mass Returned to the Saturated Zone (Vadose Zone Depth: 3 m)

decreases with increasing water infiltration is evident. All these model results are included in Appendix E.

Effect of Vadose Zone Depth

Figure 8 illustrates the effect that vadose zone depth has on the amount of mass returned to the saturated zone. The plot clearly shows that deeper vadose zones cause more mass to be delivered into the groundwater. This effect is simply due to the fact that thicker soils have a much greater potential to accumulate contaminant mass. The initial

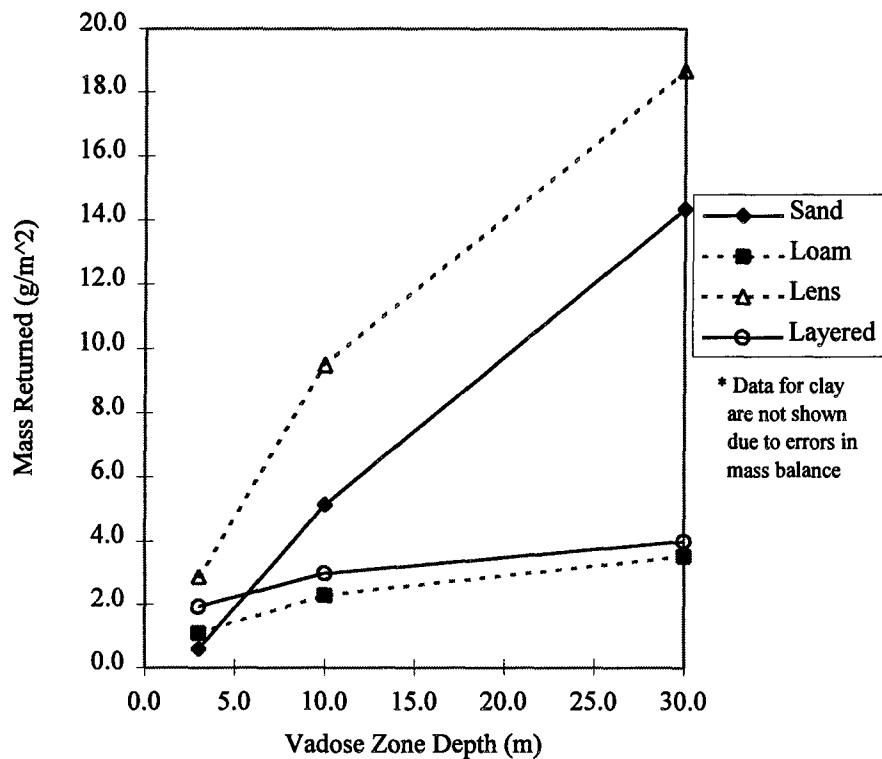


Figure 8: Effect of Vadose Zone Depth on Mass Returned to the Saturated Zone (Infiltration Rate: 0.20 cm/day)

concentration profiles displayed in Appendix C support this observation by showing a definite increase in total contaminant mass contained in the vadose zone as thicknesses increase. All the vadose zone depth results are contained in Appendix F.

Mass Fraction Returned to Saturated Zone

The information provided in the previous three sections identified how soil type, infiltration rate, and vadose zone depth effected the amount of mass returned to the saturated zone. However, in order to determine what constitutes significant

recontamination, the mass returned must be taken relative to the mass originally present in the saturated zone (see Equation 27):

$$\frac{\text{mass returned to saturated zone}}{\text{initial mass in saturated zone}} = \text{mass fraction returned} \quad (27)$$

The initial masses used in this study were calculated by assuming a sand aquifer and using a reasonable range of saturated zone thicknesses (see Equation (28)).

$$\text{initial mass in saturated zone} = \theta_s C_i (\text{saturated zone thickness}) \quad (28)$$

The mass returned data was presented previously in Tables 2 and 3; initial masses are listed in Table 4.

Table 4: Initial Mass Present in Saturated Zone

	Saturated Zone Thickness (m)					
	2.5	5.0	7.5	10.0	12.5	15.0
Mass (g/m ²)	5.21	10.43	16.64	20.85	26.06	31.28

Results illustrating the mass fraction returned to the saturated zone are provided in Appendix G. For this study, the mass fraction threshold was set at 20%. By using this threshold, each scenario was evaluated on its potential to significantly recontaminate the saturated zone. As an example, Figure 9 displays a case where significant recontamination is only likely occur when a heterogeneous soil (*Lens* or *Layered*) overlies a thin to medium saturated zone. Figure 9 also illustrates that, in this particular situation, the homogeneous soils are unlikely to pose any problem regardless of the thickness of the saturated zone. All final results are categorized in Table 5.

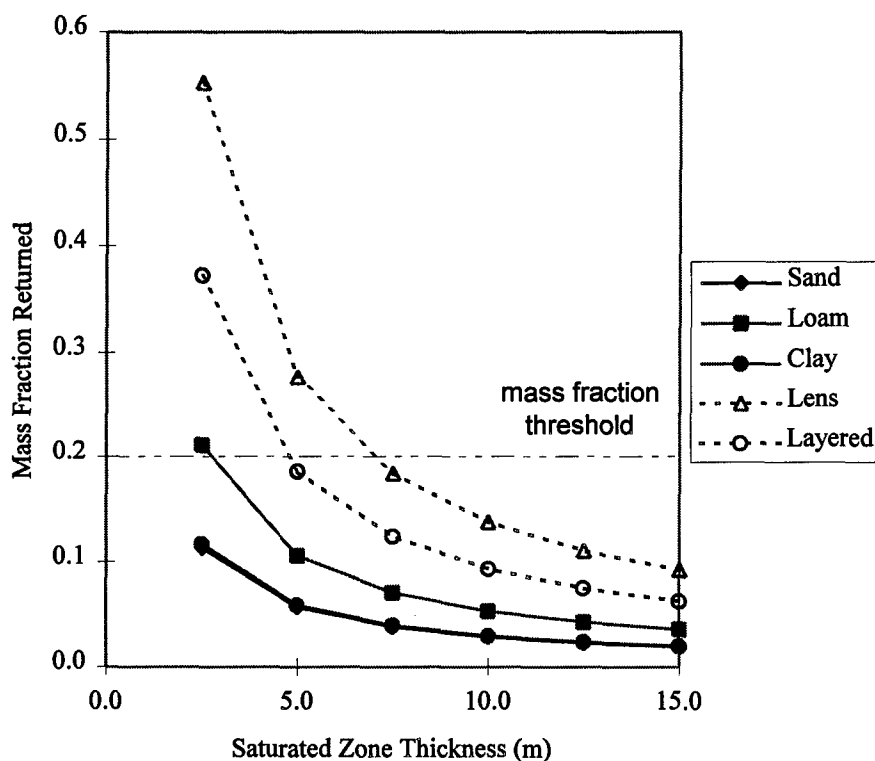


Figure 9: Mass Fraction Returned to Saturated Zone
(Infiltration Rate: 0.04 cm/day; Vadose Zone Depth: 3 m)

Fortunately, this large quantity of raw results can be reduced to a few general findings. In reference to causing significant recontamination of the saturated zone:

- 1) heterogeneous conditions are worse than homogeneous;
- 2) the presence of a low permeability layer within a highly permeable soil seems to be the worst case situation;
- 3) low infiltration rates are worse than high (as long as zero is not approached);
- 4) deep vadose zones are worse than shallow; and,
- 5) thin saturated zones are worse than thin

For a more quantitative perspective, the reader is directed to Table 5 or to Appendix G to obtain specific information on a particular issue.

Table 5: Final Results for All Scenarios

Infil Rate (cm/day)	Sand			Loam			Vadose Zone Depth
	Saturated Zone Thickness ¹			Saturated Zone Thickness ¹			
	Thin	Medium	Thick	Thin	Medium	Thick	
0.00	N	N	N	N	N	N	Shallow (3 m)
0.04	N	N	N	N	N	N	
0.20	N	N	N	N	N	N	
0.40	M	N	N	N	N	N	
0.00	S	S	N	N	N	N	Moderate (10 m)
0.04	S	S	M	S	M	N	
0.20	S	S	S	S	N	N	
0.40	S	S	S	S	N	N	
0.00	S	S	S	S	M	N	Deep (30 m)
0.04	S	S	S	S	M	N	
0.20	-----	-----	-----	-----	-----	-----	
0.40	S	S	S	-----	-----	-----	

Infil Rate (cm/day)	Clay ²			Vadose Zone Depth
	Saturated Zone Thickness			
	Thin	Medium	Thick	
0.00	S	M	N	Shallow (3 m)
0.04	S	M	N	
0.20	S	M	N	
0.40	M	N	N	

Notation

- S Significant recontamination (mass factor returned > threshold)
- M Marginal recontamination (mass factor returned < threshold {interval crosses threshold})
- N No recontamination (mass factor returned < threshold)
- Result exhibited mass significant balance errors

¹ General thicknesses: thin: 2.5 - 5.0 m; medium: 5.0 - 10.0 m; thick: 10.0+ m

² Results for clay with medium and deep vadose zones exhibited significant mass balance errors

Table 5: Final Results for All Scenarios (cont'd)

Infil Rate (cm/day)	Lens			Layer			Vadose Zone Depth
	Saturated Zone Thickness			Saturated Zone Thickness			
	Thin	Medium	Thick	Thin	Medium	Thick	
0.00	S	M	N	S	N	N	Shallow (3 m)
0.04	S	M	N	S	N	N	
0.20	S	M	N	M	N	N	
0.40	M	N	N	----	----	----	
0.00	S	S	S	S	S	N	Moderate (10 m)
0.04	S	S	S	S	M	N	
0.20	----	----	----	S	M	N	
0.40	----	----	----	S	M	N	
0.00	S	S	S	S	M	N	Deep (30 m)
0.04	S	S	S	S	M	N	
0.20	----	----	----	----	----	----	
0.40	----	----	----	----	----	----	

Note: Notation is defined in the first part of this table

Effect of Model Boundary Conditions

It was suspected that the use of unrealistically abrupt lower boundary conditions in the model might have induced substantially large contaminant fluxes across the water table. Since in the natural environment, contaminant concentrations rise and fall gradually, the concern was that the model might significantly overestimate mass transport. To determine the extent to which the abrupt boundary conditions effected model output, four selected scenarios were ran using a different set of boundary conditions. The new boundary conditions caused the aqueous concentration to linearly rise from zero to the specified level gradually over 200 days (vadose zone contamination phase). Subsequently, for the recontamination phase, the concentration fell gradually to

zero over another 200 days. Model results using these new gradient boundary conditions are located in Appendix H.

Table 6 provides a comparison of the mass fractions returned under each boundary condition scheme.

Table 6: Effect of Boundary Conditions on Mass Fraction Returned
(Infiltration Rate: 0.04 cm/day; Vadose Zone Depth: 30 m)

Soil Type	Mass Fraction Returned		% Change
	Abrupt BC	Gradient BC	
Sand	14.34	13.47	6.1
Loam	3.53	3.43	2.8
Lens	18.66	17.83	4.4
Layered	3.99	----- ^a	N/A

^a Result exhibited significant mass balance errors

The small percent changes shown in Table 6 imply that the choice of boundary conditions do not significantly effect the model's outcome. The reason for this is apparent from Figure 10 which compares the fluxes of the two boundary condition schemes. Despite greatly different fluxes at short times, the overall area under the two flux curves appears to be very comparable. As a result, total masses determined by integration of these curves would be similar and not greatly change model results.

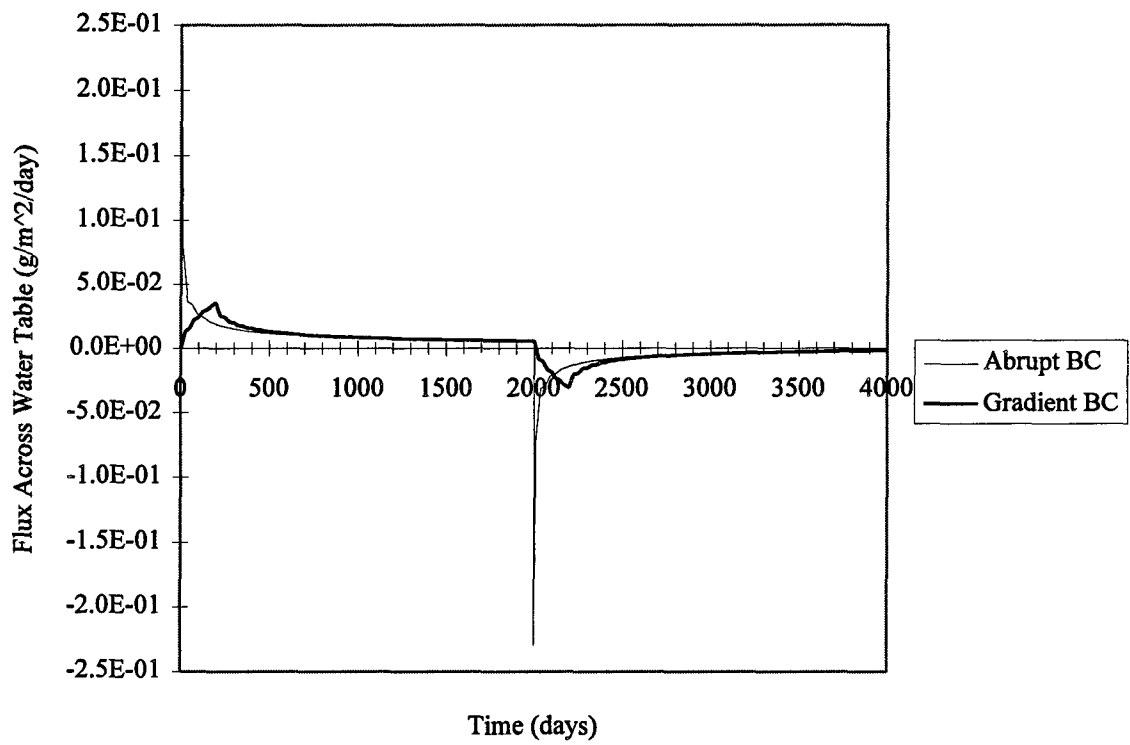


Figure 10: Effect of Boundary Conditions on Flux Across Water Table
 (Soil Type: Sand; Infiltration Rate: 0.04 cm/day; Vadose Zone Depth: 30 m)

V. Conclusions

Summary of Significant Findings

This study had two purposes: (1) to determine the fate of VOCs which migrate into the vadose zone from the saturated zone, and (2) to determine conditions where VOCs in the vadose zone could cause significant recontamination of groundwater. The task was accomplished by modeling the transport of TCE between the saturated and vadose zones using differing soil types, water infiltration rates, and vadose zone depths.

In general, model results indicated that only a small fraction of the total contaminant mass escaped into the atmosphere or remained in the vadose zone. The majority of the contaminant mass was transported back into the saturated zone. Soil type, infiltration rate, vadose zone depth, and saturated zone thickness, all had a substantial effect on the magnitude of recontamination. Deep, heterogeneous soil profiles accompanied with low infiltration rates posed the greatest threat to saturated zone contamination. Moreover, the presence of a low permeability lens in a highly porous soil seemed to create the worst case. Additionally, most water infiltration rates actually decreased recontamination of the groundwater by minimizing the migration of VOCs into the vadose zone.

Recommendations for Future Research

Since, this study was limited one dimension, it would be interesting to develop a multi-dimensional model and/or incorporate more realistic boundary conditions to determine if the results significantly change. Efforts to validate the model against existing field or experimental data are also necessary.

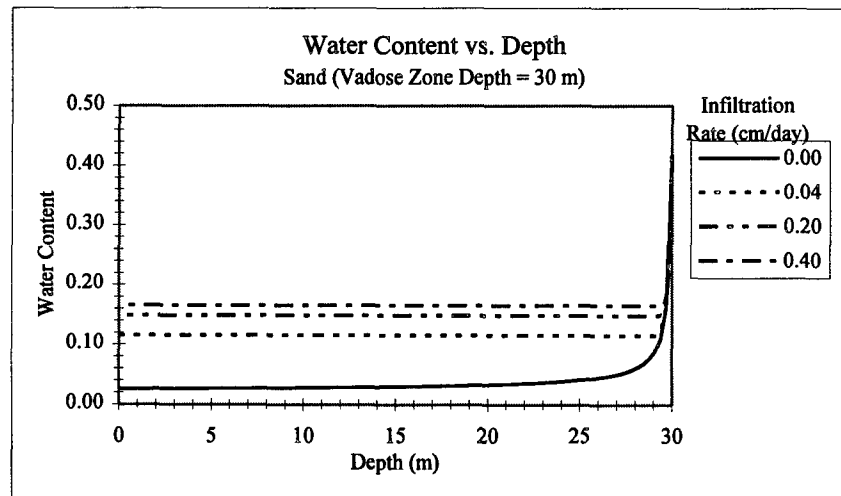
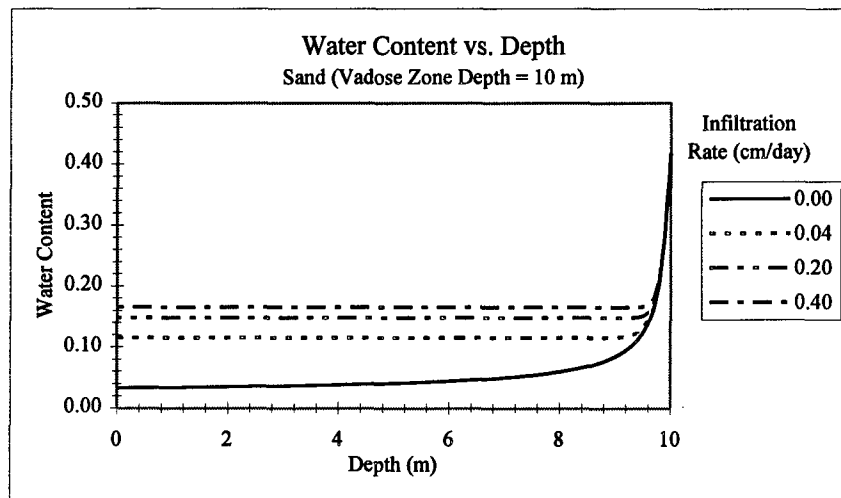
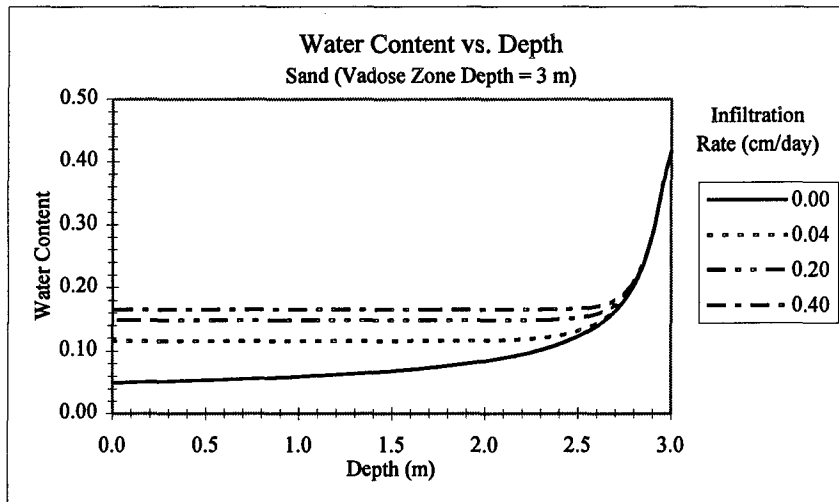
Appendix A: Notation

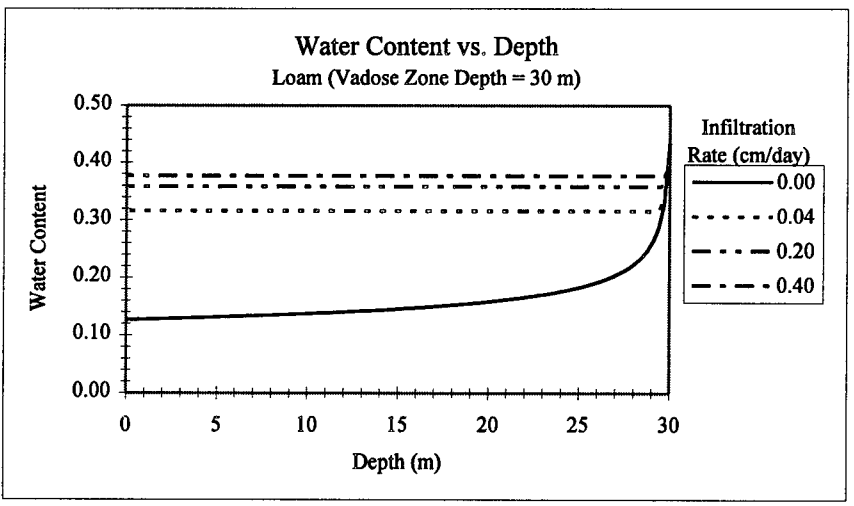
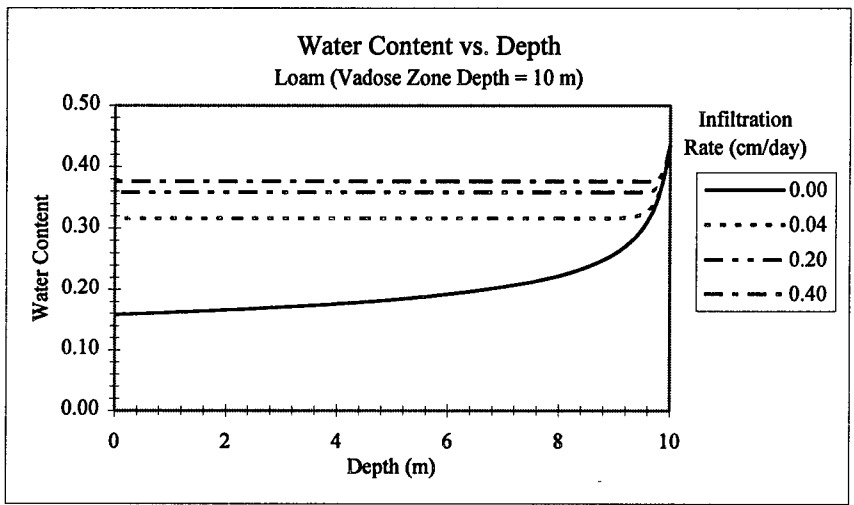
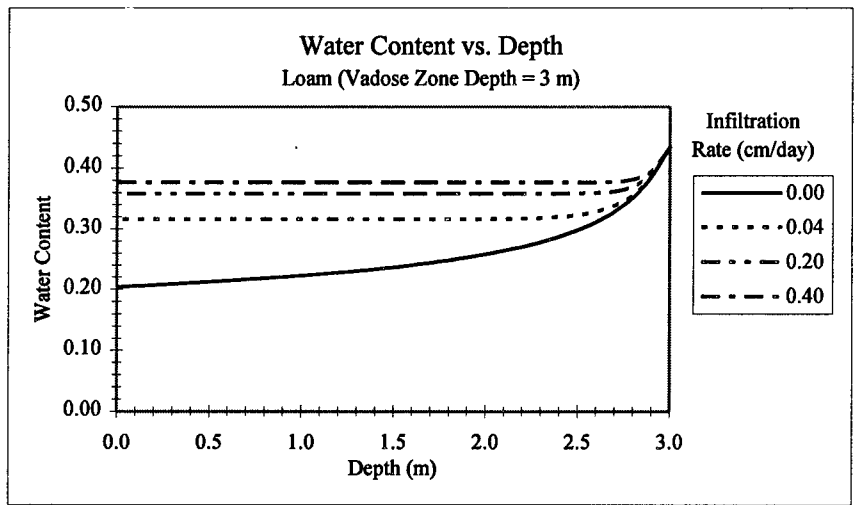
Symbol	Description	Dimension*
C_a	Solute concentration in gaseous (air) phase	$[M L_a^{-3}]$
C_i	Initial aqueous phase solute concentration in saturated zone	$[M L_w^{-3}]$
C_s	Solute concentration in soil phase due to aqueous phase sorption	$[M M_s^{-1}]$
C_w	Solute concentration in aqueous phase	$[M L_w^{-3}]$
D_a	Effective gaseous phase diffusion-dispersion coefficient	$[L^2 T^{-1}]$
D_w	Effective aqueous phase diffusion-dispersion coefficient	$[L^2 T^{-1}]$
D_{fa}	Free air molecular diffusion coefficient	$[L^2 T^{-1}]$
D_{fw}	Free water molecular diffusion coefficient	$[L^2 T^{-1}]$
h	Hydraulic head	$[L]$
h_b	Bubbling pressure (Brooks and Corey soil parameter)	$[L]$
J	Solute flux	$[M L^{-2} T]$
J_{srf}	Solute flux across soil surface	$[M L^{-2} T]$
J_{wt}	Solute flux across water table	$[M L^{-2} T]$
K	Unsaturated hydraulic conductivity	$[L T^{-1}]$
K_s	Saturated hydraulic conductivity	$[L T^{-1}]$
K_d	Solids/Water distribution coefficient	$[L_w^3 M_s^{-1}]$
K_H	Henry's law constant (air/water partitioning coefficient)	[unitless]
L	Total depth of vadose zone	$[L]$
m	Van Genuchten soil parameter	[unitless]
n	Effective porosity	[unitless]
q_{wz}	Vertical aqueous phase advective flux through vadose zone	$[L T^{-1}]$
q_{wx}	Horizontal aqueous phase advective flux through saturated zone	$[L T^{-1}]$
z	Depth	$[L]$
α	Van Genuchten soil parameter	$[L^{-1}]$
α_L	Longitudinal dispersivity in vadose zone	$[L]$
α_T	Transverse dispersivity in vadose zone (from groundwater flow)	$[L]$
β	Van Genuchten soil parameter	[unitless]
θ_a	Volumetric air content	[unitless]
θ_r	Residual volumetric water content	[unitless]
θ_s	Saturated volumetric water content	[unitless]
θ_w	Volumetric water content	[unitless]
λ	Pore-size distribution index (Brooks and Corey soil parameter)	[unitless]
ρ_b	Solids bulk density	$[M_s L_m^{-3}]$
τ_a	Gaseous phase tortuosity factor	[unitless]
τ_w	Aqueous phase tortuosity factor	[unitless]
Ψ	Pressure head	$[L]$

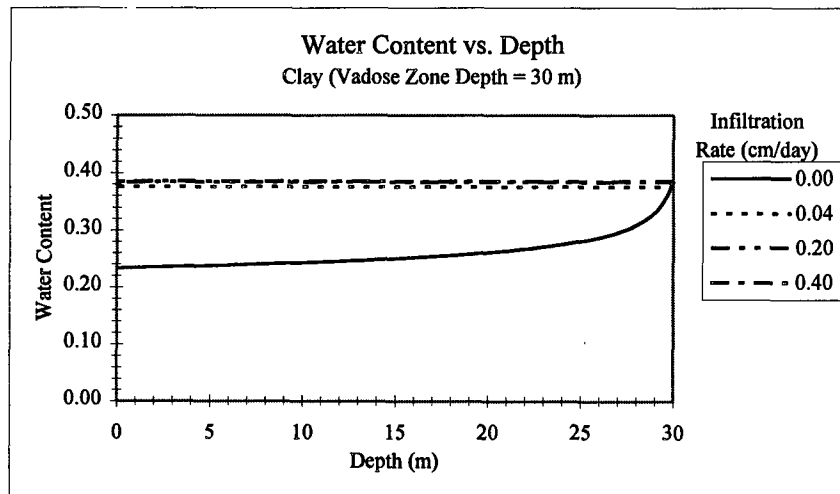
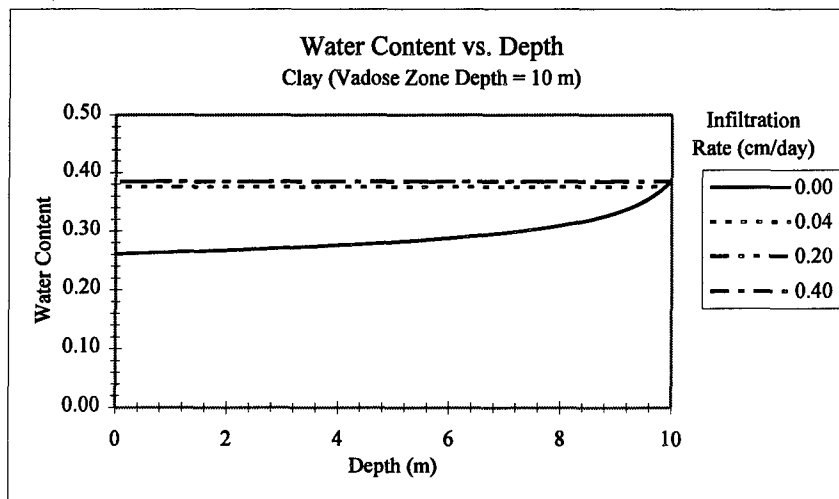
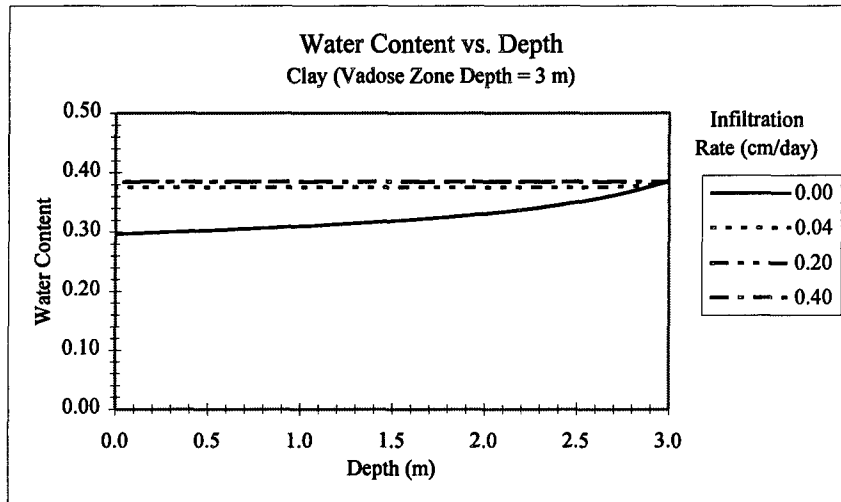
* Dimensions: L = length
 M = mass
 T = time

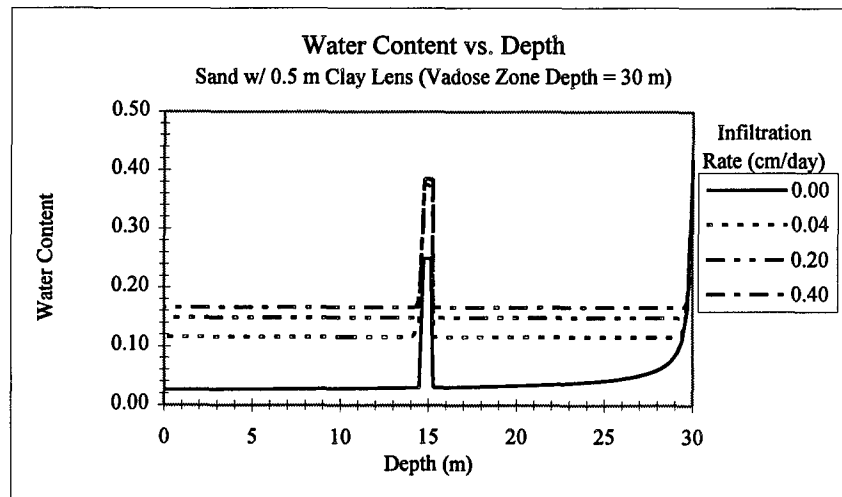
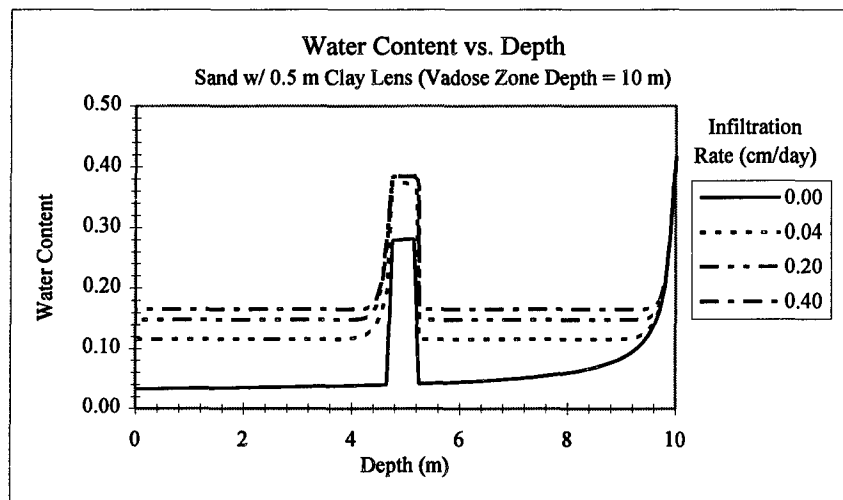
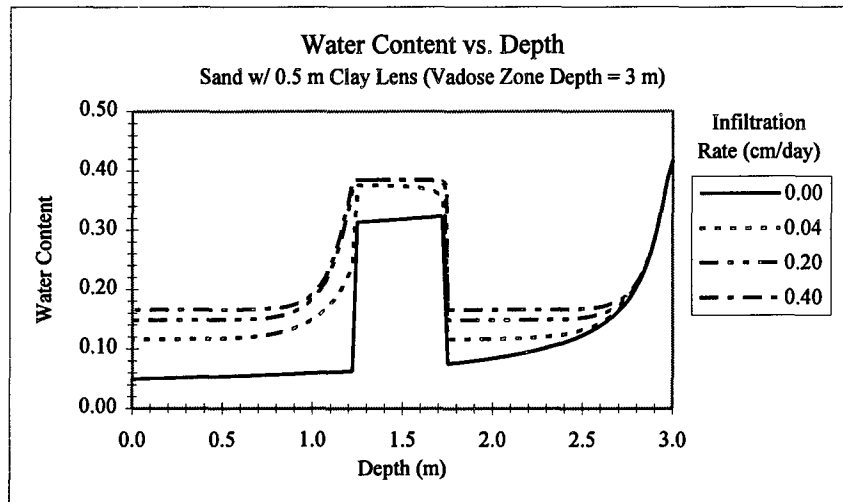
Dimension subscripts: a = air v = voids
 m = media w = water
 s = solids

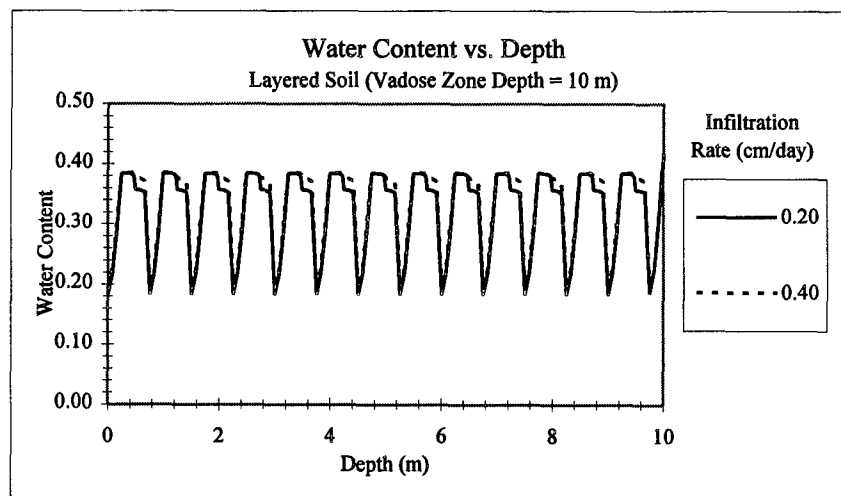
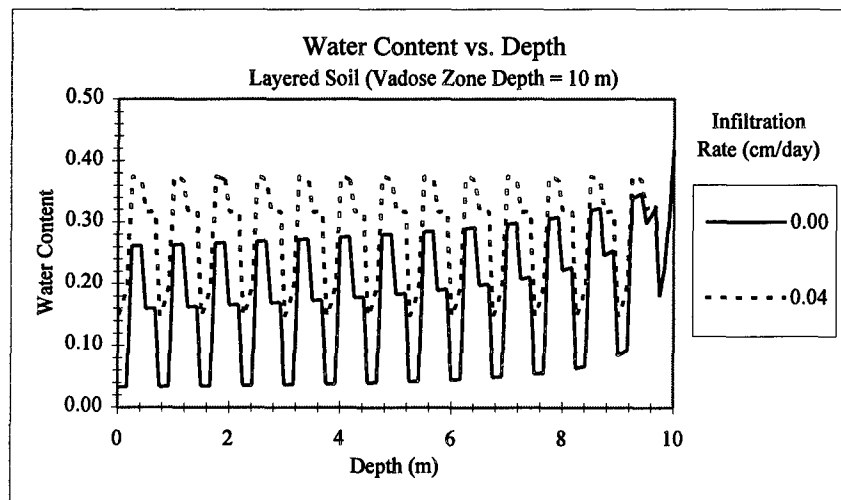
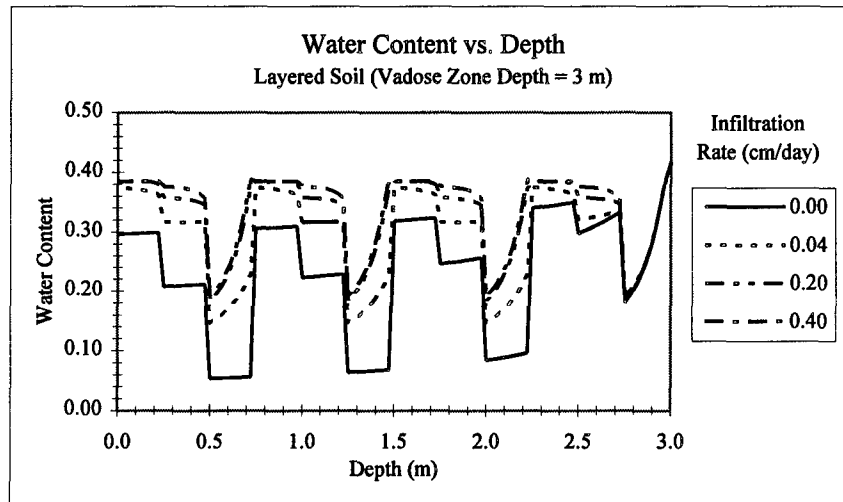
Appendix B: Soil Water Content Profiles

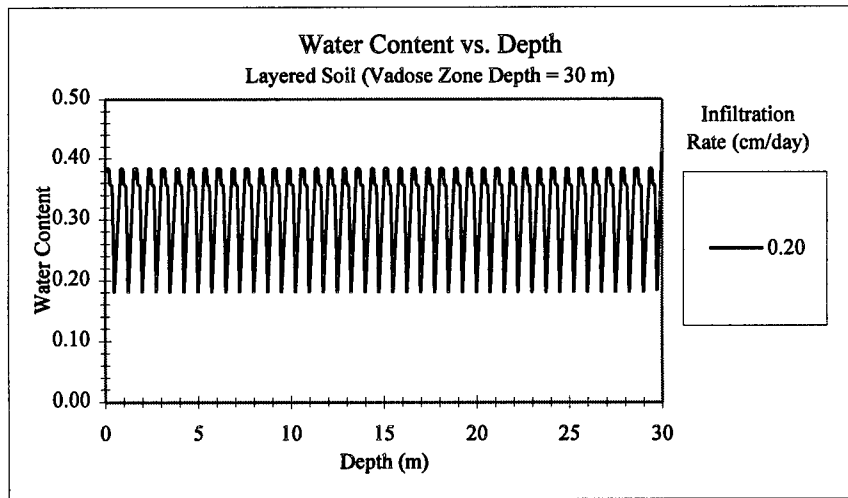
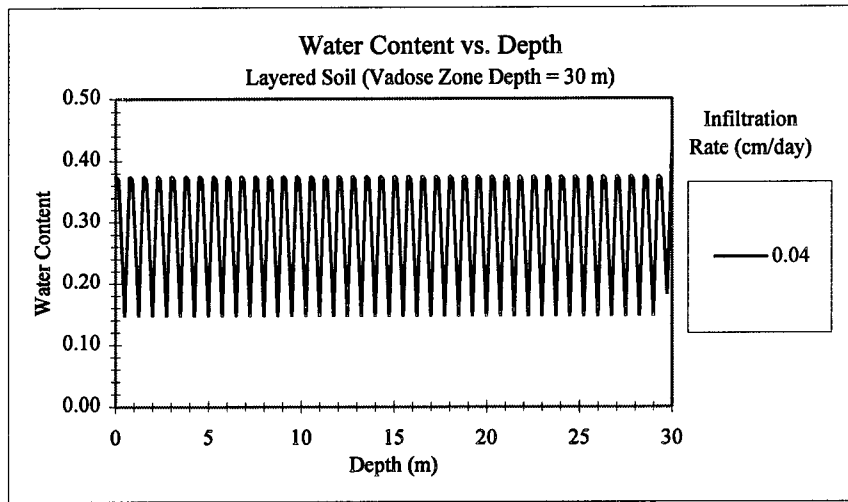
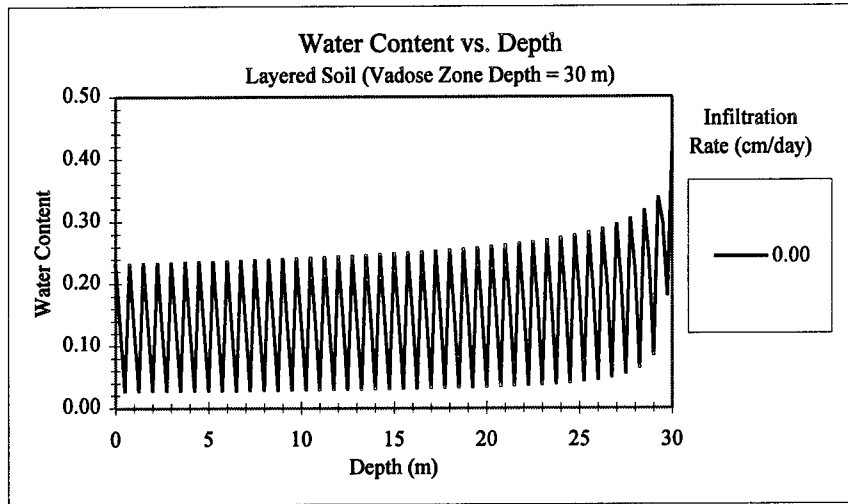


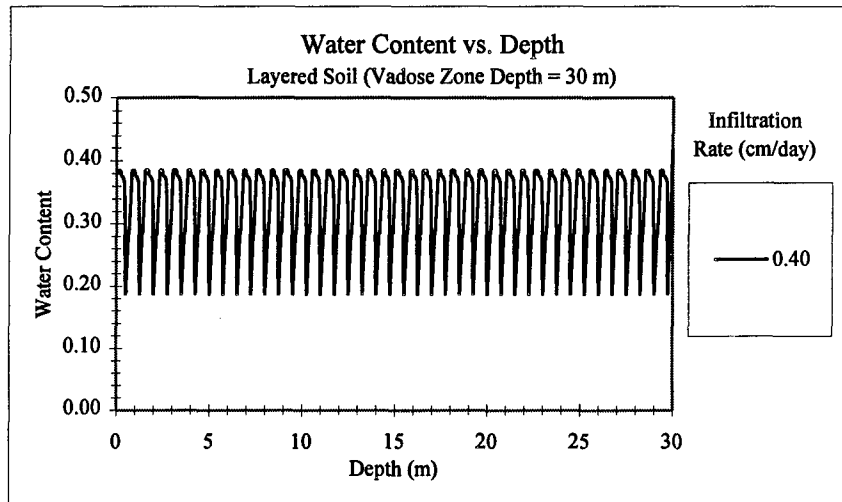




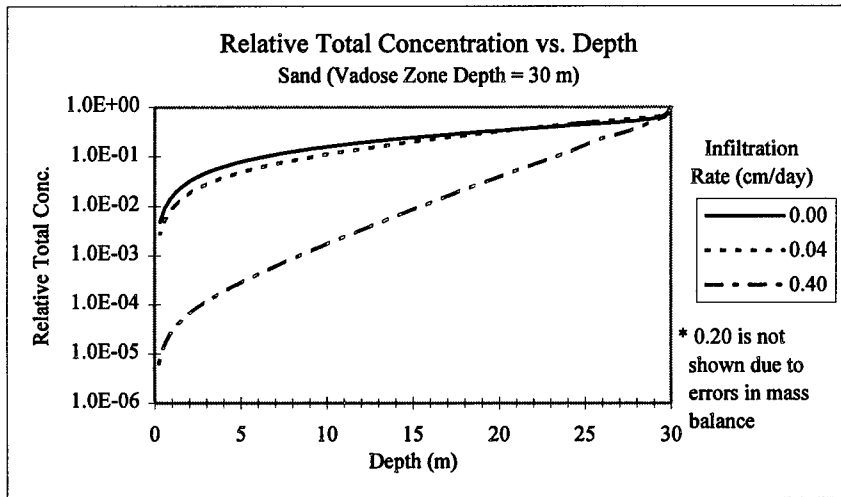
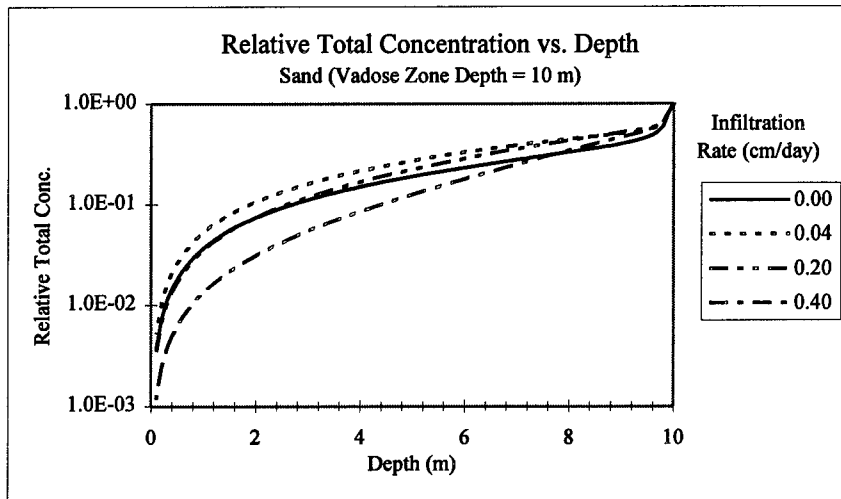
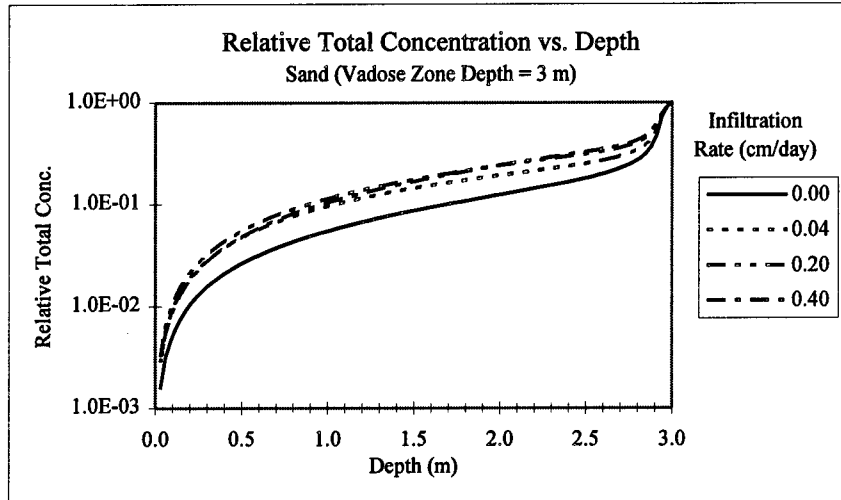


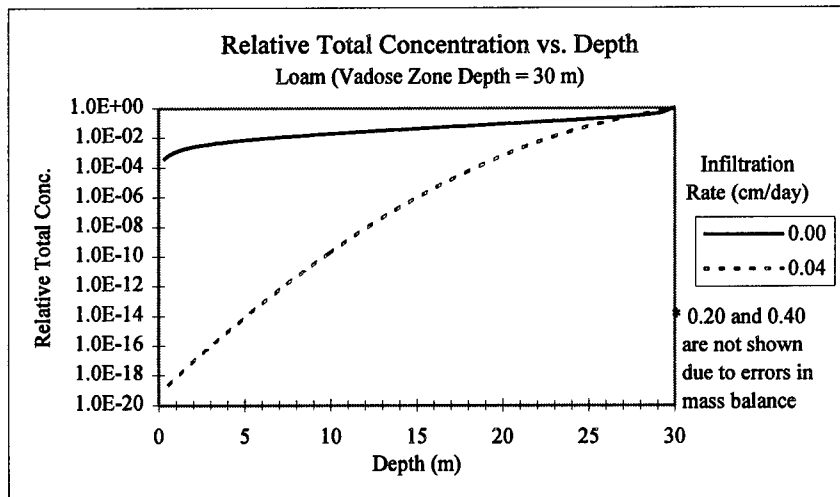
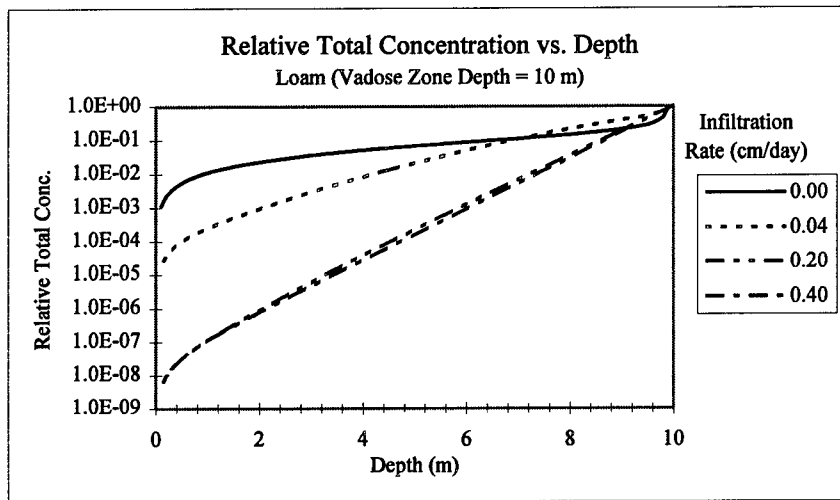
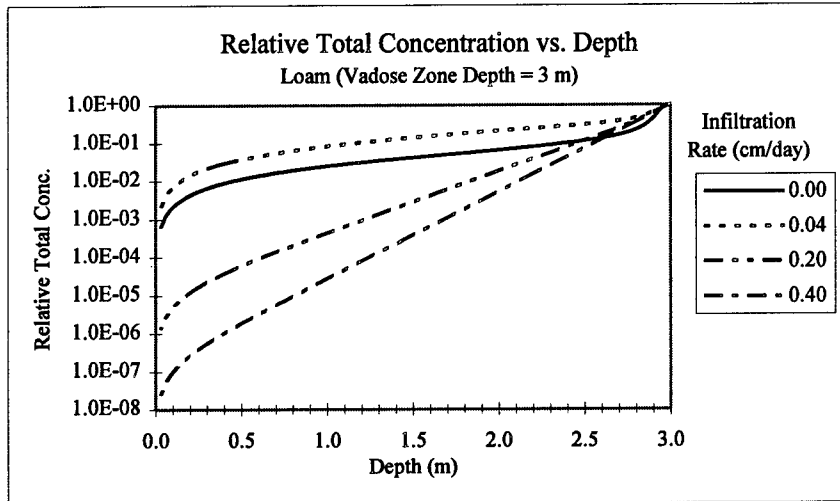


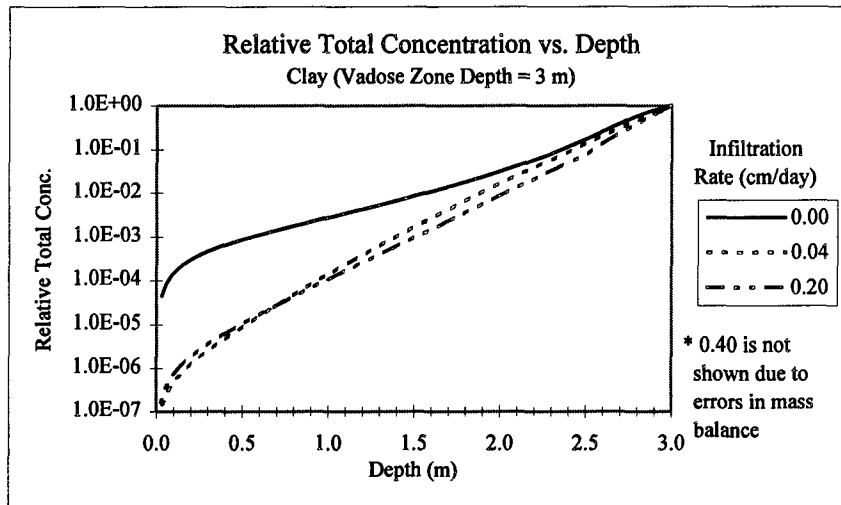




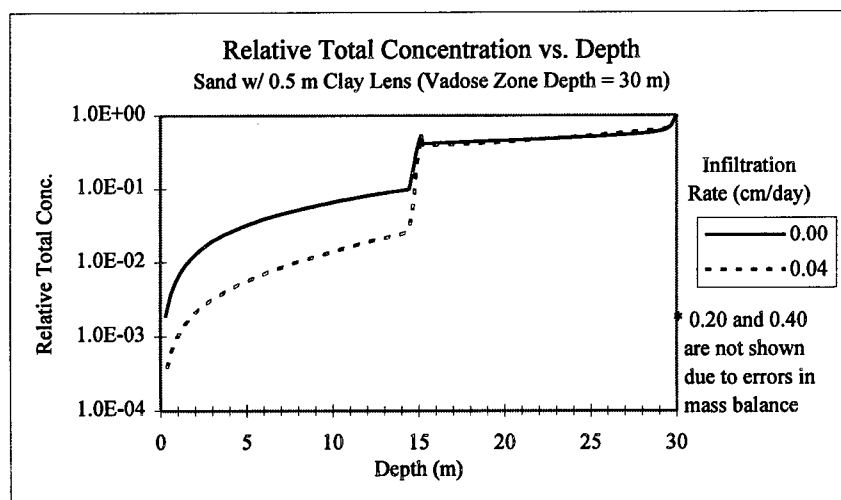
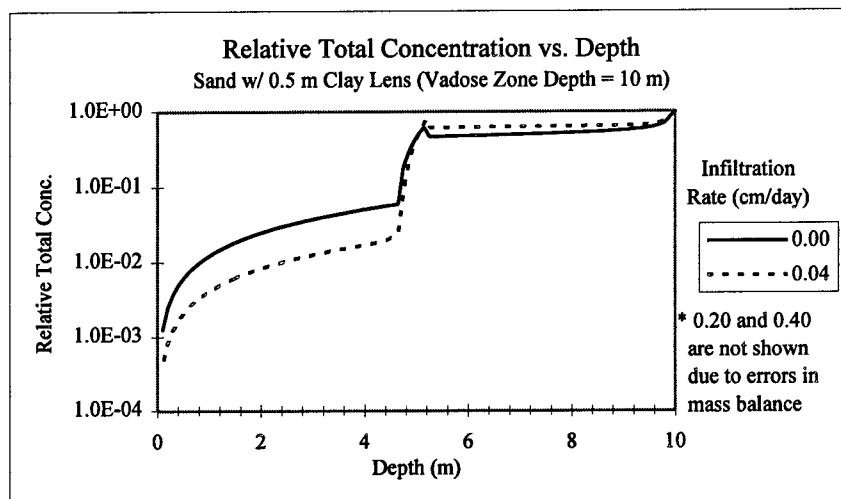
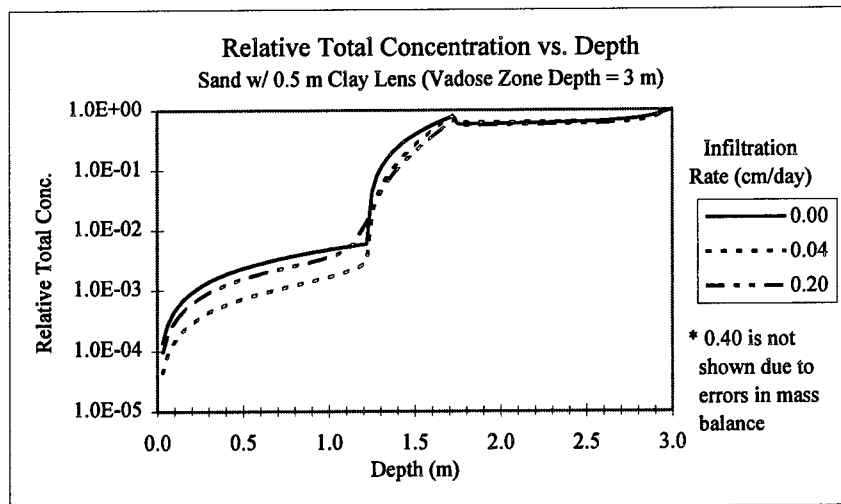
Appendix C: Initial Vadose Zone Concentration Profiles

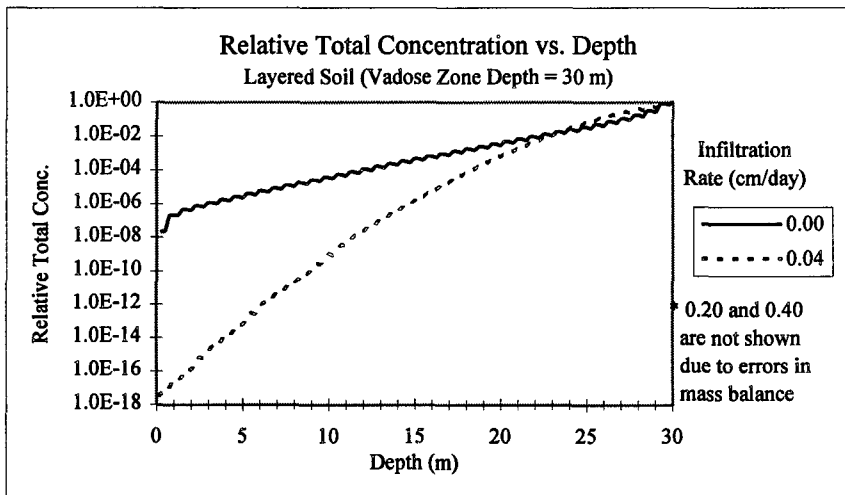
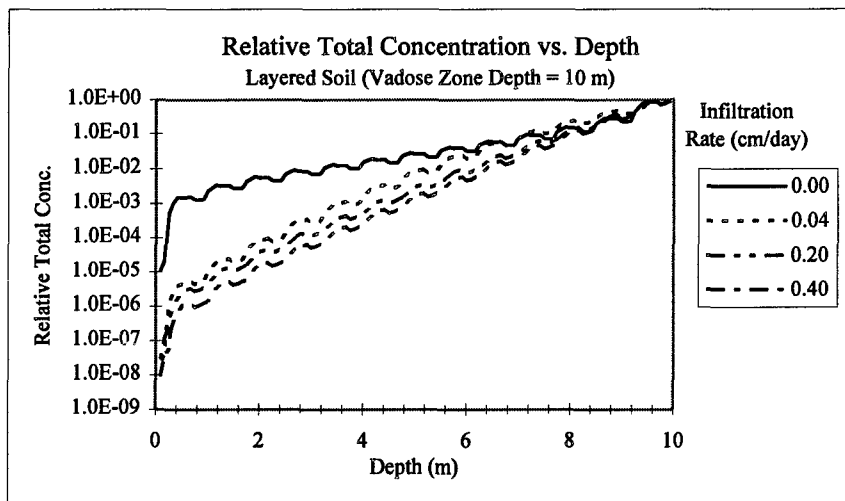
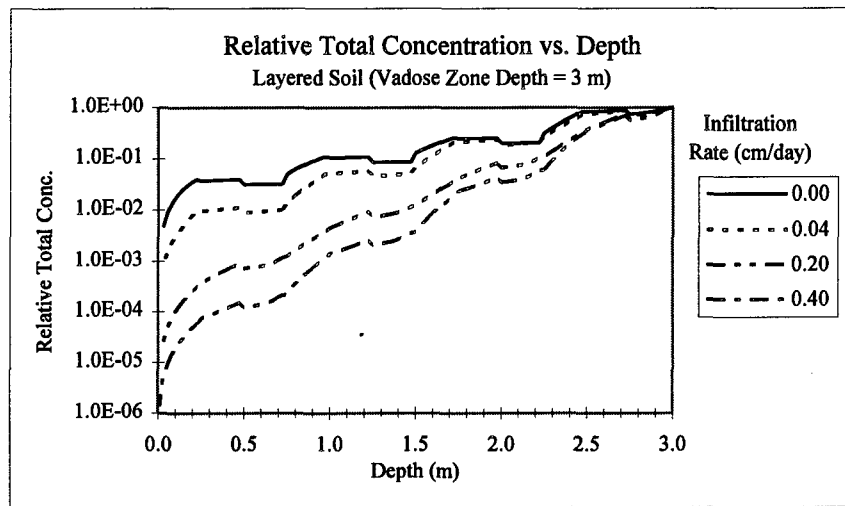




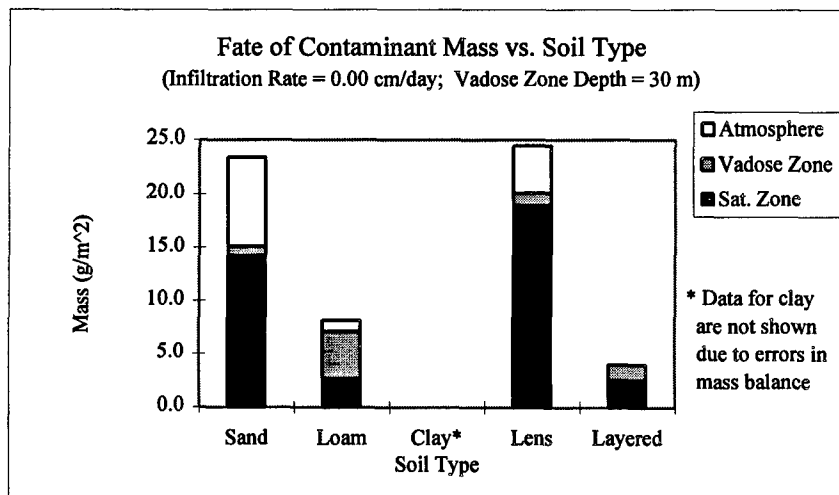
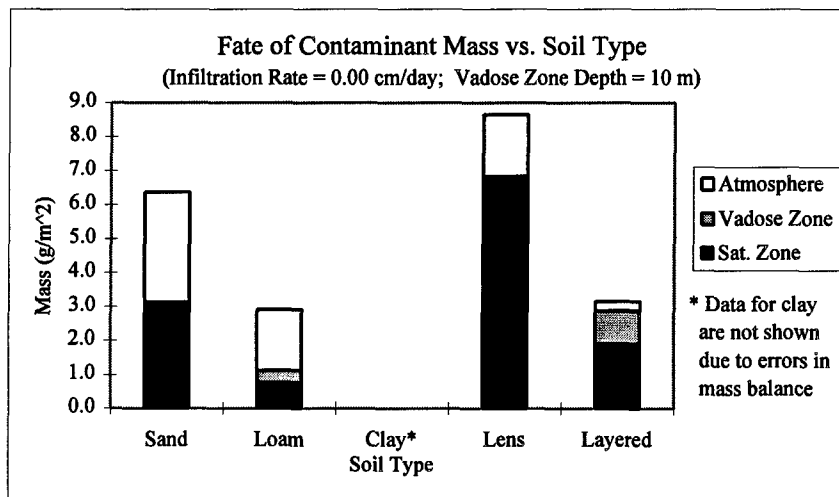
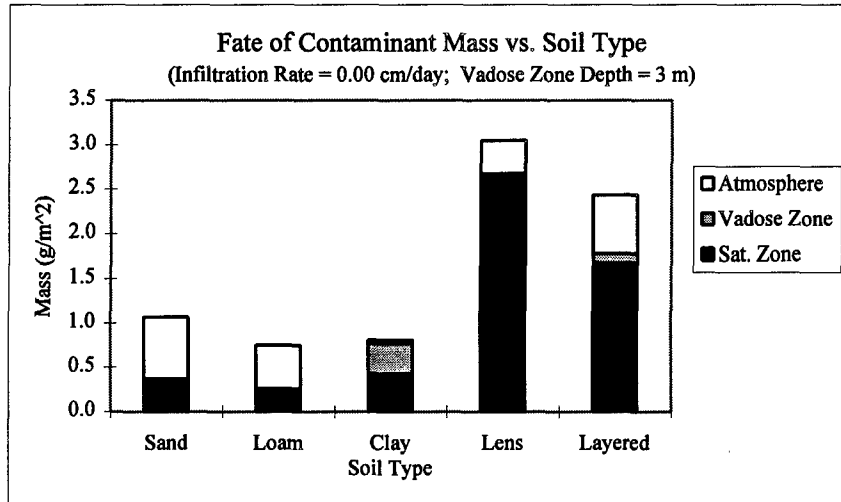


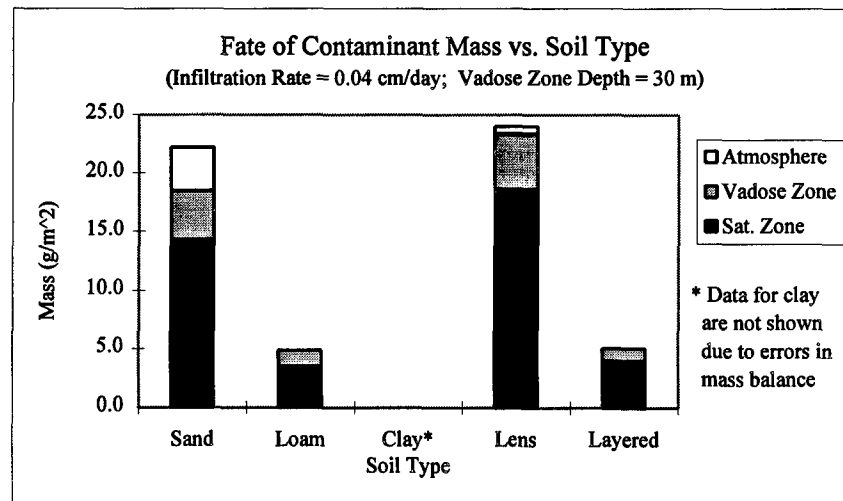
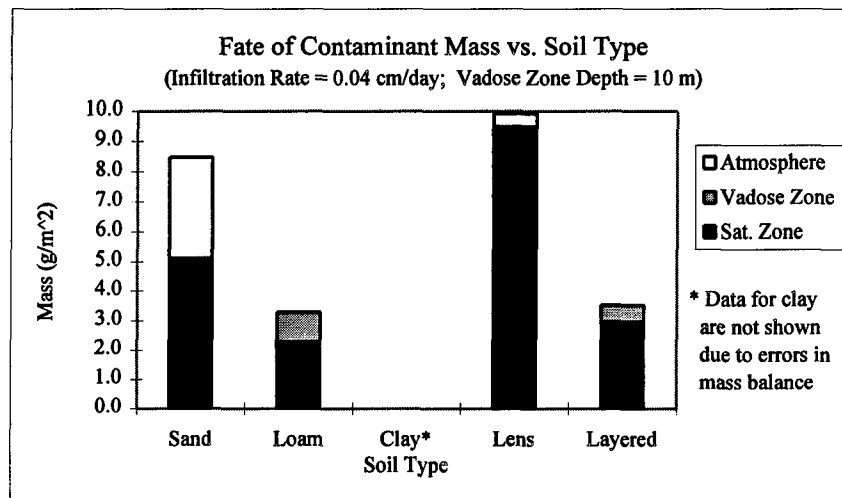
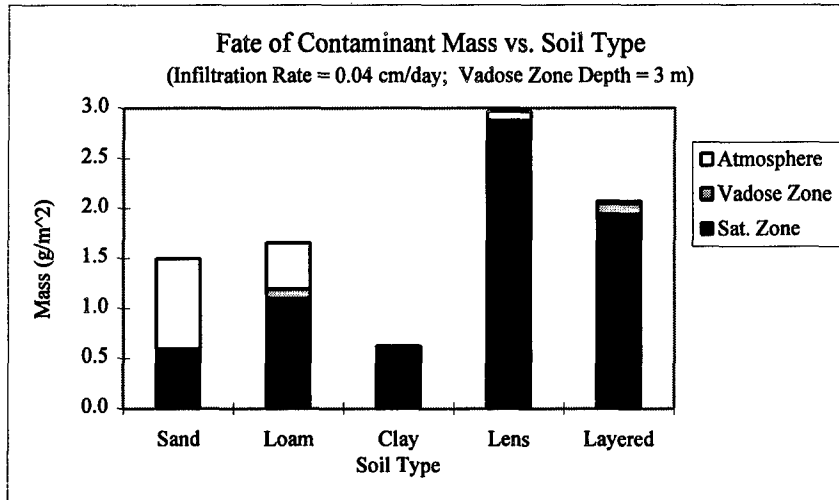
Not shown are the concentration profiles for clay with vadose zone depths of 10 and 30 m. Those cases exhibited significant mass balance errors.

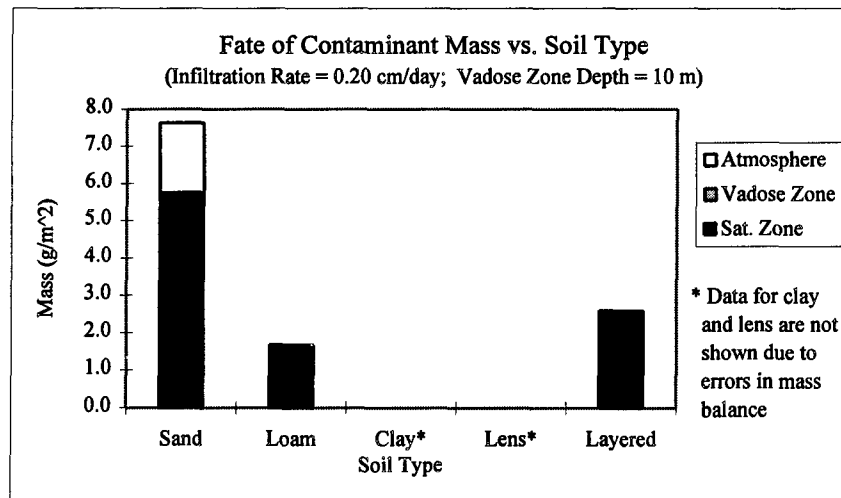
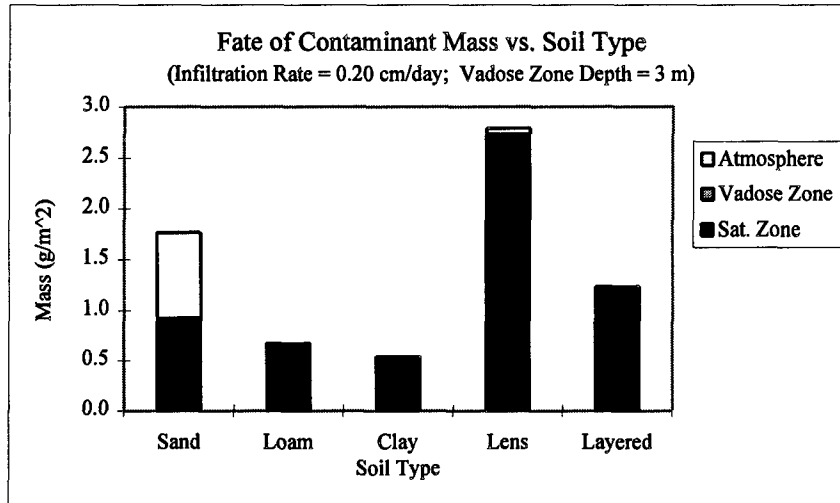




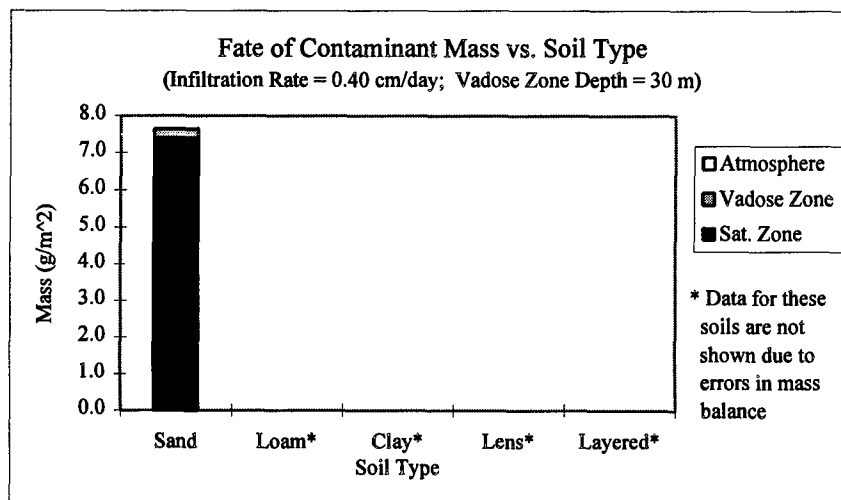
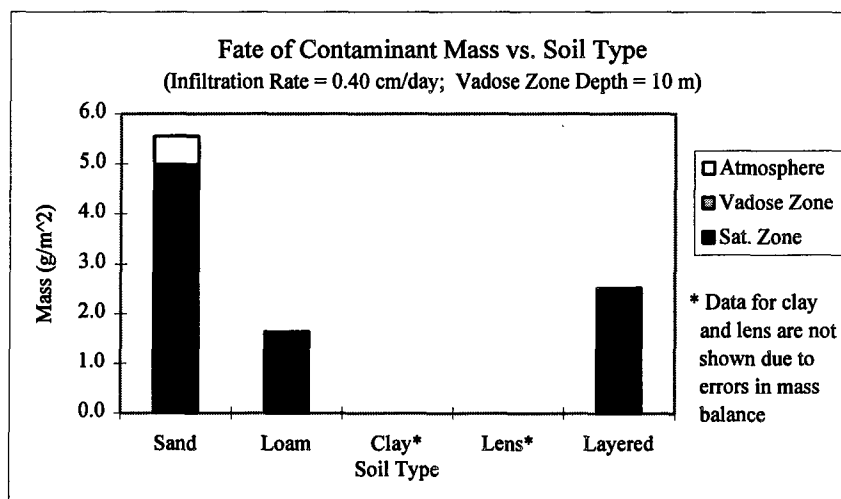
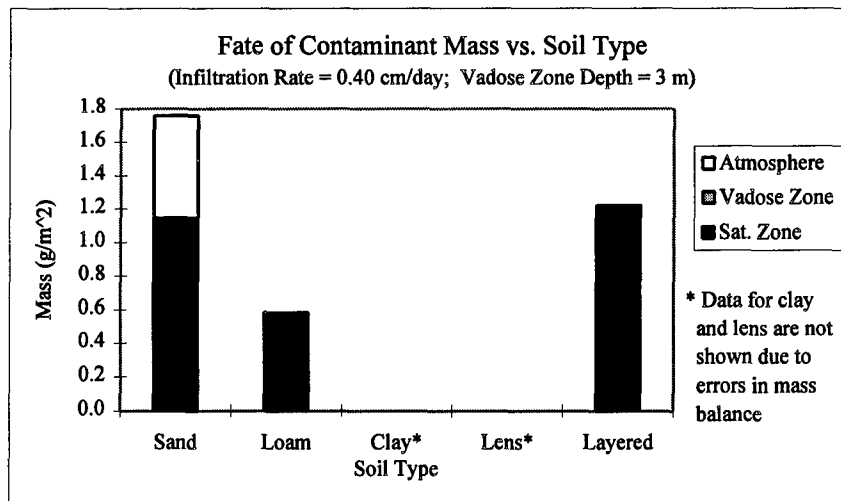
Appendix D: Effect of Soil Type on Contaminant Fate



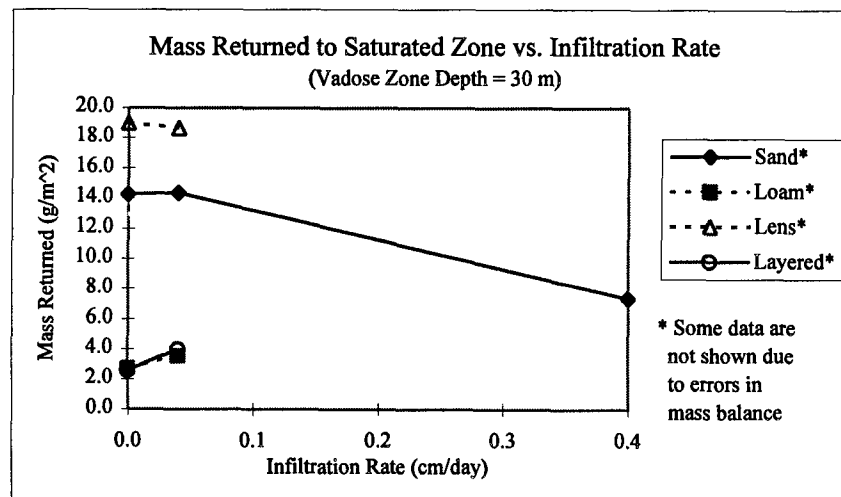
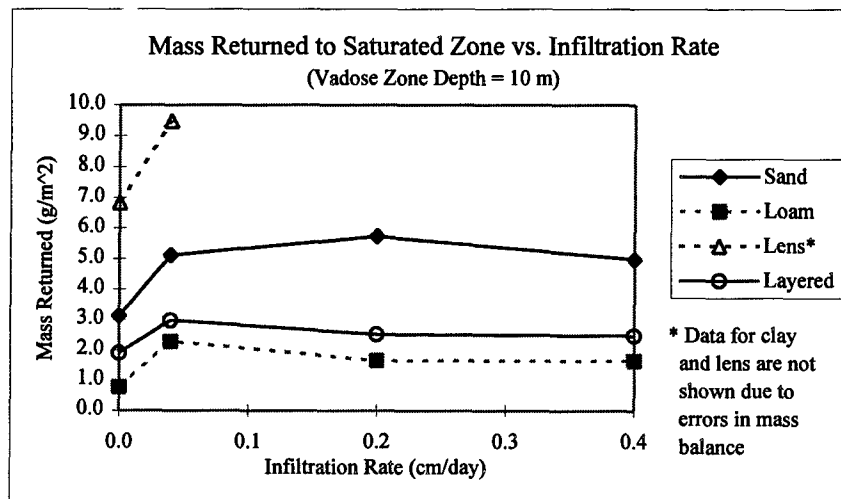
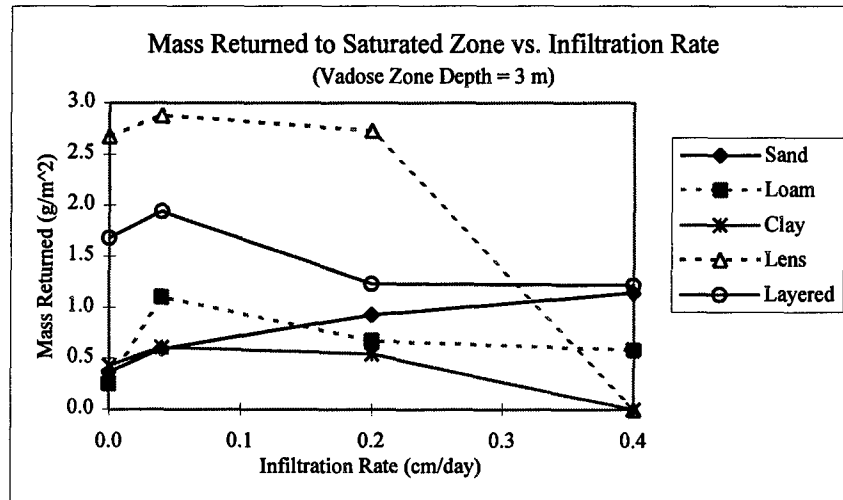




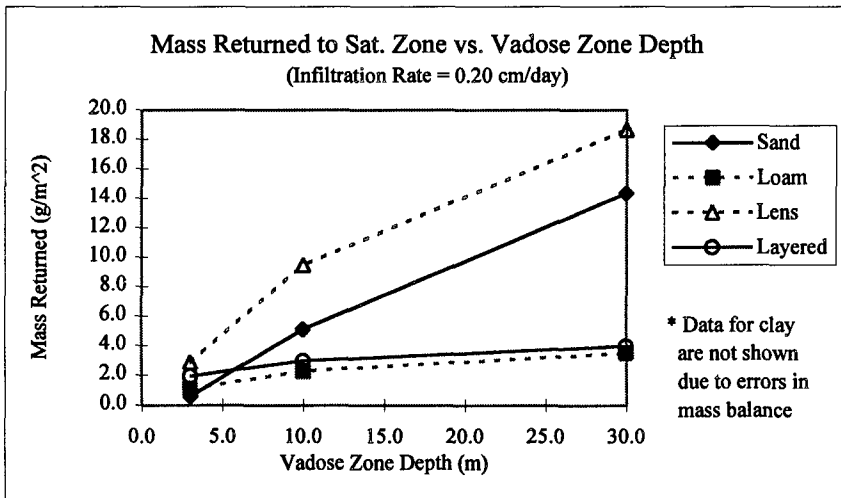
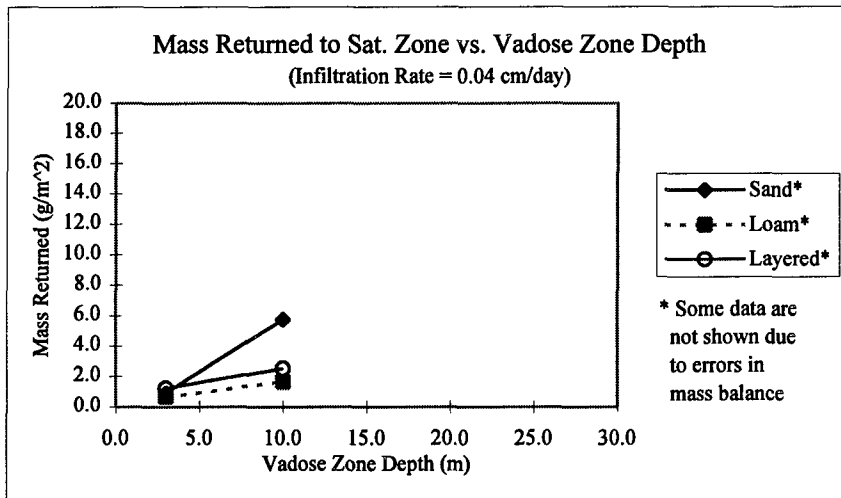
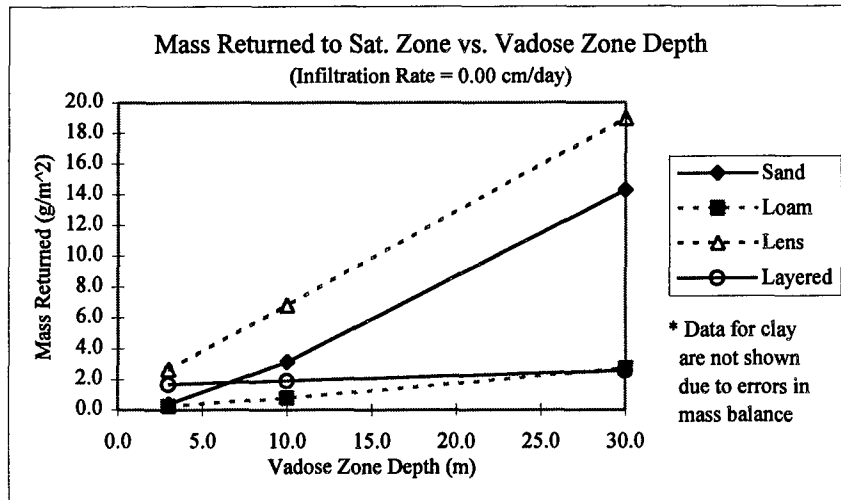
Not shown are the results with an infiltration rate of 0.20 cm/day and a vadose zone depth of 30. For this case, all soils exhibited significant mass balance errors.

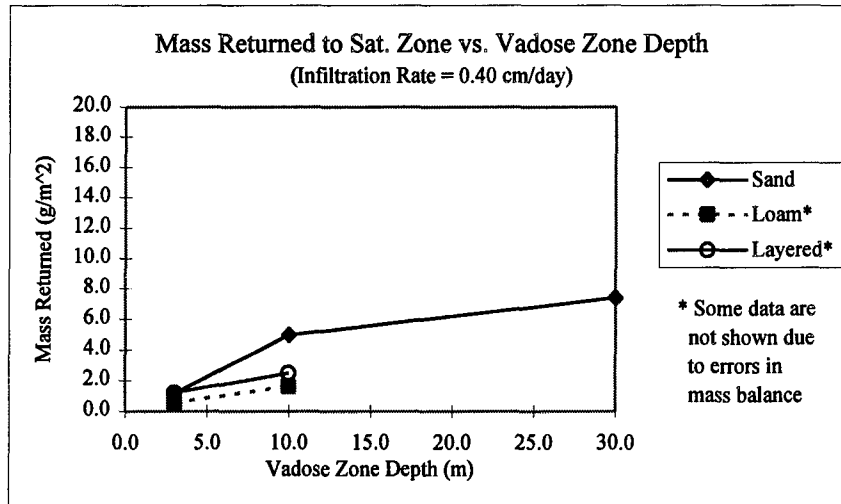


Appendix E: Effect of Infiltration Rate on Saturated Zone Recontamination

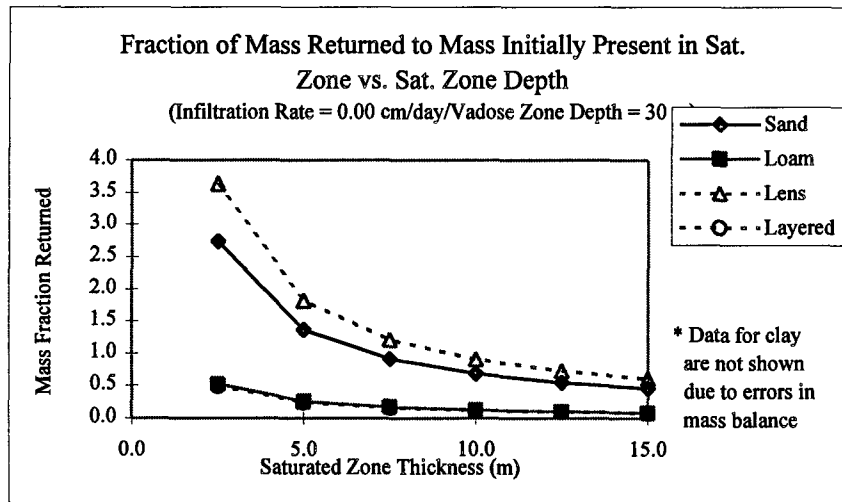
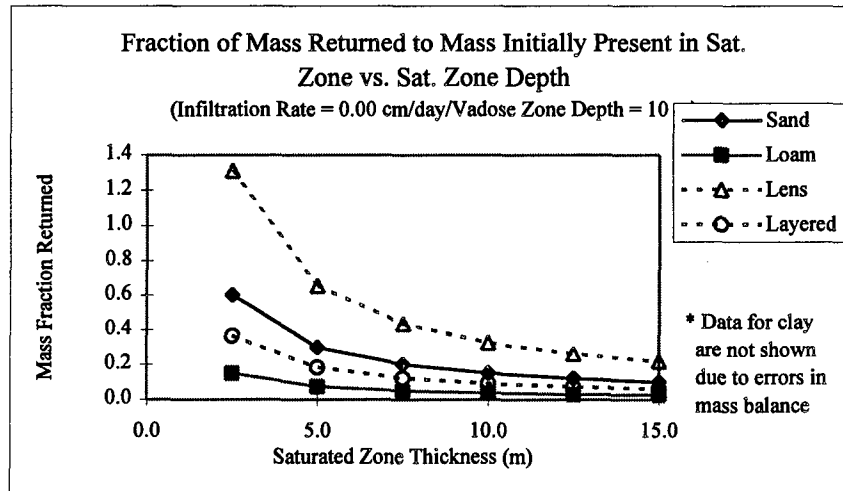
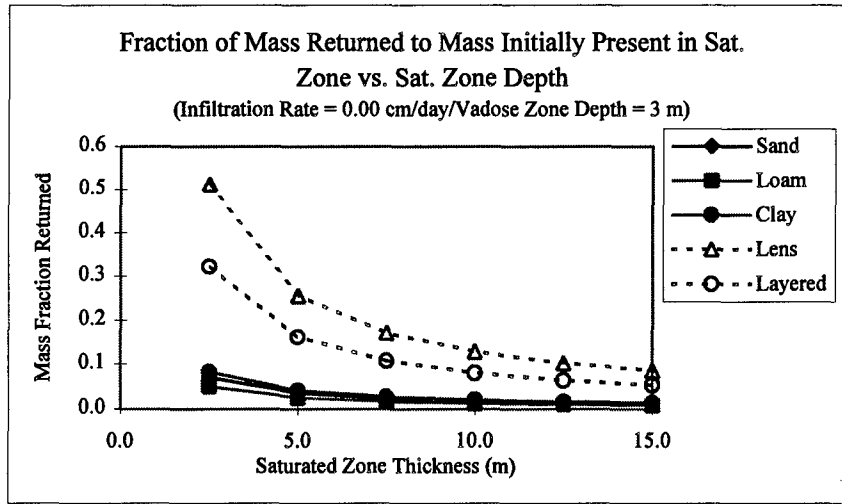


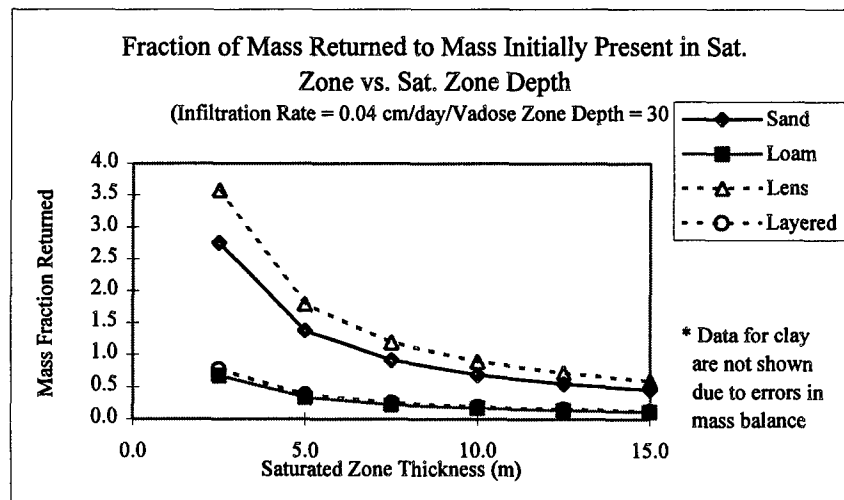
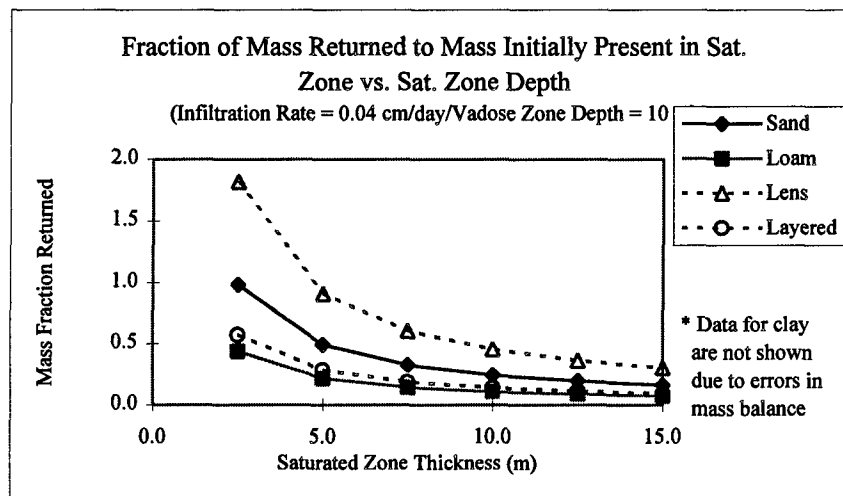
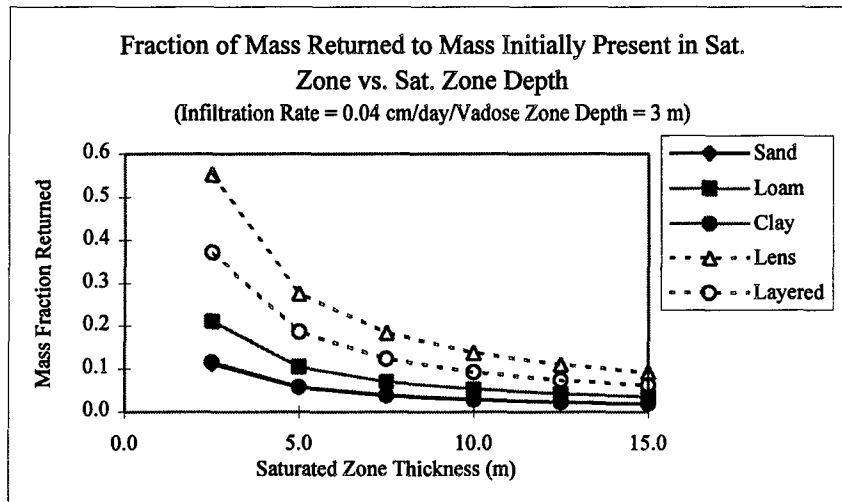
Appendix F: Effect of Vadose Zone Depth on Saturated Zone Recontamination

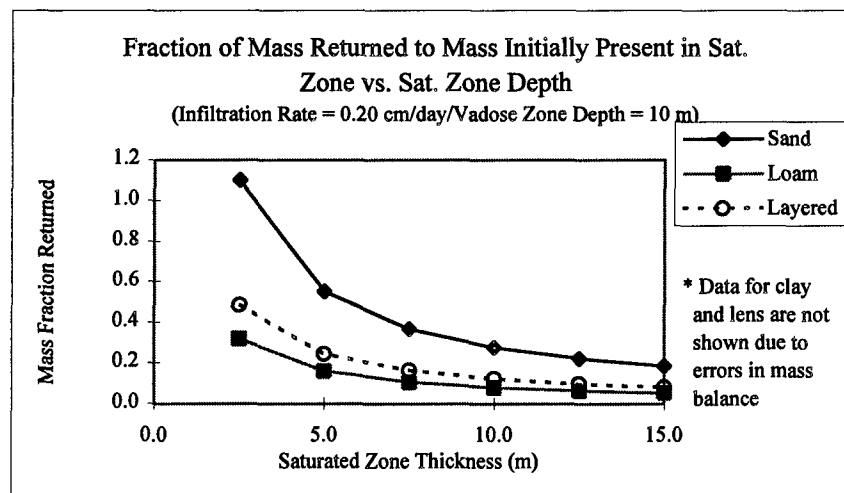
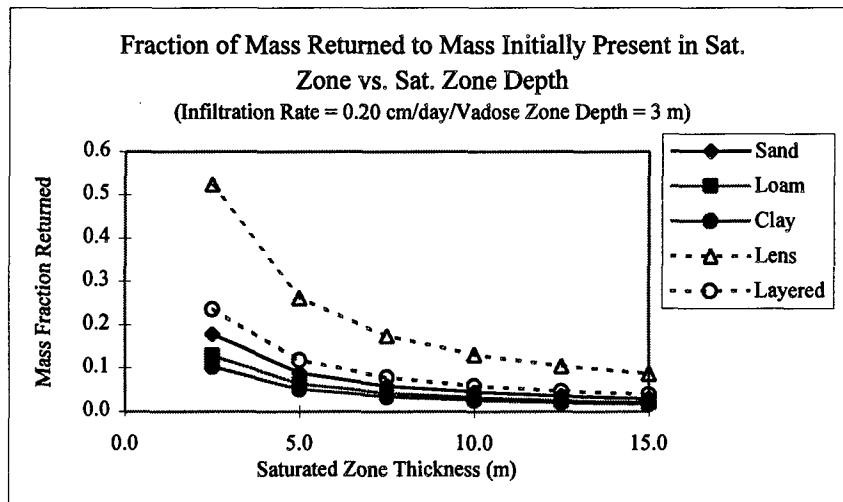




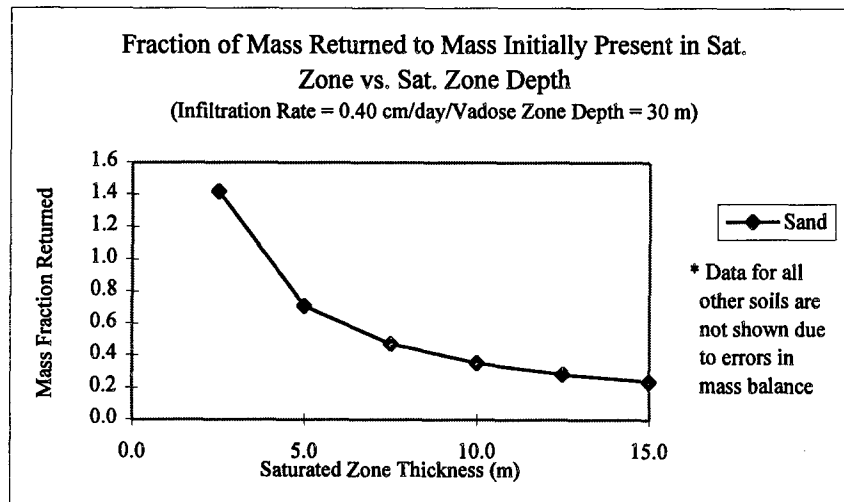
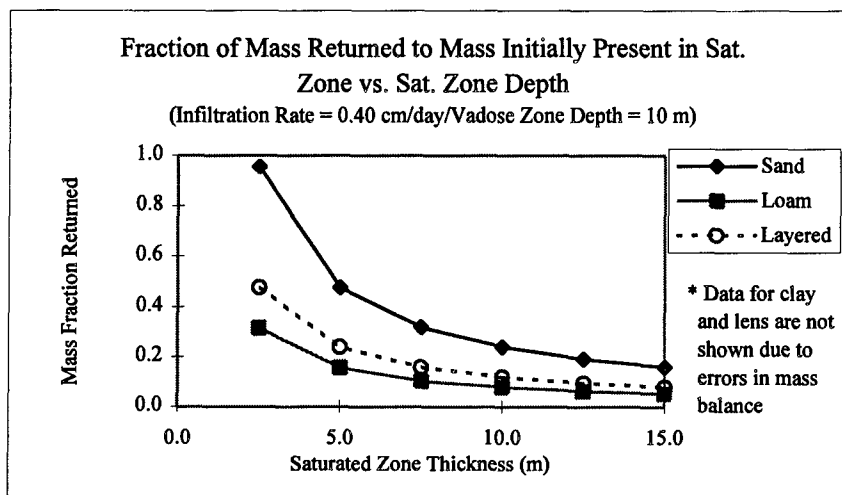
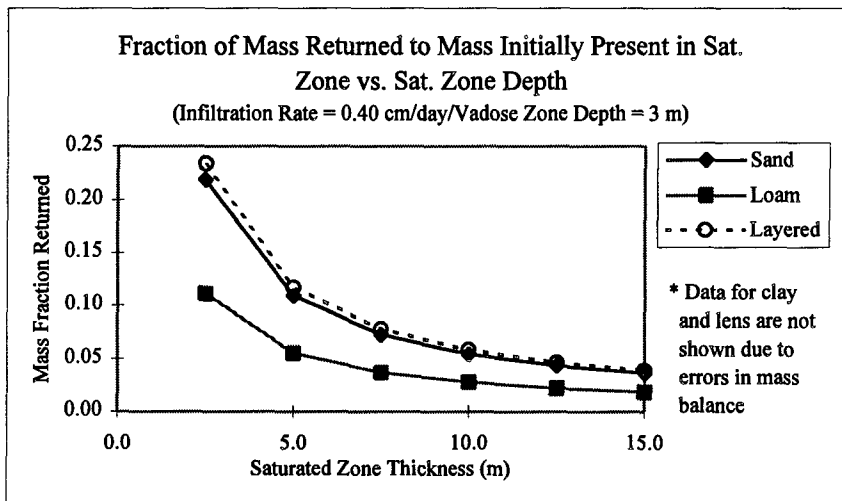
Appendix G: Mass Fraction Returned to the Saturated Zone





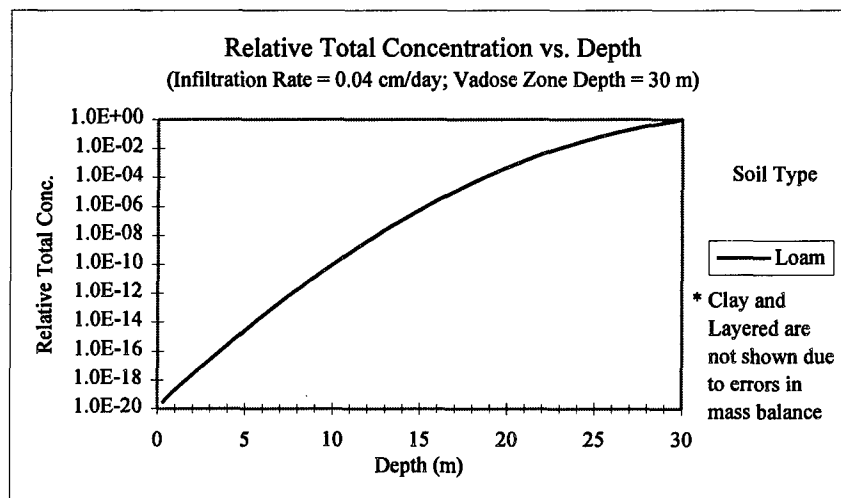
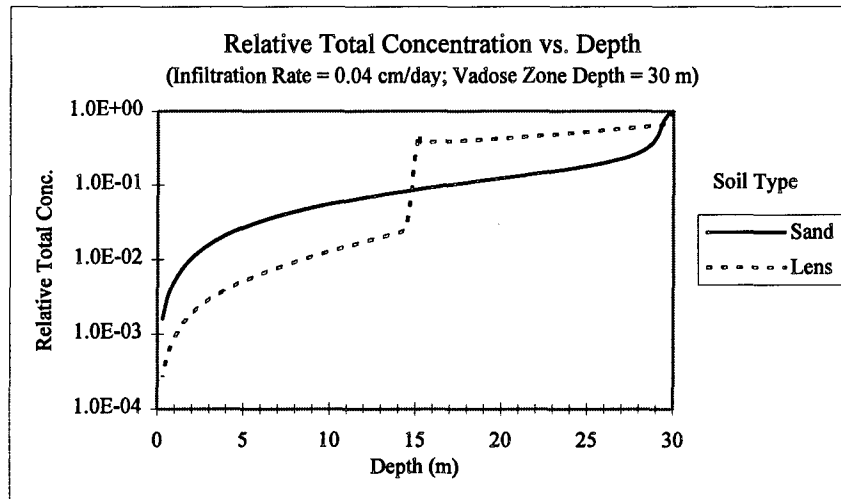


Not shown are the results with an infiltration rate of 0.20 cm/day and a vadose zone depth of 30. For this case, all soils exhibited significant mass balance errors.



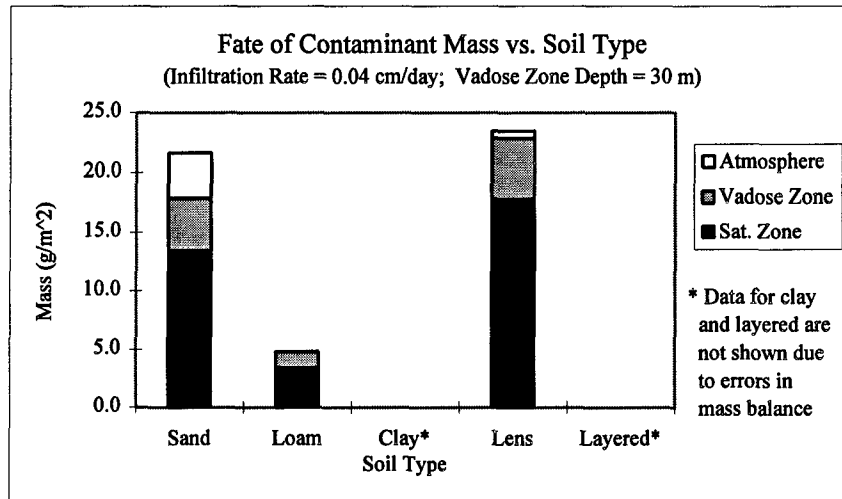
Appendix H: Results Using Gradient Boundary Conditions

Initial Vadose Zone Concentration Profiles:



Not shown are the concentration profiles for the clay and layered cases which exhibited significant mass balance errors.

Effect of Soil Type on Contaminant Fate:



Appendix I: Equation Development for Soil Water Content Model

1. Apply Buckingham Equation to define $\Psi(z)$:

a. Assumptions:

1. Discontinuous porous medium can be described by a hypothetical continuous representative elementary volume (REV)
2. One dimensional laminar flow
3. Porous media is homogeneous, isotropic, isothermic, and nondeformable
4. Fluids are incompressible (densities of water and air are constant)
5. Steady state
6. Velocity head is negligible

b. Equation Development:

$$q_{wz} = -K(\Psi) \frac{\partial h}{\partial z} \quad \text{where: } h = \Psi + z \quad (\text{Buckingham, 1907})$$

$$q_{wz} = -K(\Psi) \left(\frac{\partial(\Psi)}{\partial z} + 1 \right)$$

c. Finite-difference approximation to be solved iteratively for $\Psi(z)$:

$$-K(\Psi_{avg}) \left(\frac{\Psi_{i+1} - \Psi_i}{\Delta z} + 1 \right) = q_{wz}$$

where:

$$\Psi_{avg} = \frac{\Psi_{i+1} + \Psi_i}{2}$$

$$K(\Psi_{avg}) = \frac{K_s \left[1 - (\alpha \Psi_{avg})^{\beta-1} \left[1 + (\alpha \Psi_{avg})^\beta \right]^{-m} \right]^2}{\left[1 + (\alpha \Psi_{avg})^\beta \right]^{\frac{m}{2}}} \quad (\text{van Genuchten, 1980})$$

$$\alpha = (h_b)^{-1} \quad \beta = \lambda + 1 \quad m = \frac{\lambda}{\lambda + 1}$$

d. Boundary Condition: $\Psi(z = L) = 0$

2. Solve for $\theta_w(z)$:

$$\theta_w(z) = \theta_r + \frac{\theta_s - \theta_r}{\left[1 + [\alpha\Psi(z)]^\beta\right]^m}$$

(van Genuchten, 1980)

Appendix J: Equation Development for Contaminant Transport Model

1. Fundamental Mass Transport and Flux Equations for the Unsaturated Zone:

a. Assumptions:

1. Discontinuous porous medium can be described by a hypothetical continuous representative elementary volume (REV)
2. One dimensional laminar flow
3. Fluids are incompressible (densities of water and air are constant)
4. No NAPL phase present
5. Vapor sorption is negligible
6. Air phase is passive (gaseous advective flux is negligible)
7. All other sources and sinks are negligible

b. Contaminant Transport Equation:

$$\frac{\partial}{\partial t}(\theta_w C_w + \theta_a C_a + \rho_b C_s) = -\frac{\partial}{\partial z}(q_{wz} C_w) + \frac{\partial}{\partial z}\left(D_w \frac{\partial C_w}{\partial z} + D_a \frac{\partial C_a}{\partial z}\right)$$

c. Flux Equation:

$$J = q_{wz} C_w - D_w \frac{\partial C_w}{\partial z} - D_a \frac{\partial C_a}{\partial z}$$

2. Simplify Equation:

a. Assumptions:

1. Porous media is homogeneous, isotropic, and isothermic (D_{fw} , D_{fa} , ρ_b , and n are constant in space)
2. Porous media is nondeformable (ρ_b and n are constant in time)
3. Steady state vertical water flow (q_{wz} and is constant with time and space; θ_w and θ_a are constant in time)
4. Local equilibrium
5. Solids/water distribution and air/water partitioning are linear:

$$C_s = K_d C_w$$

$$C_a = K_H C_w \quad (\text{assuming ideal behavior} \Rightarrow \text{aqueous activity coefficient} = 1)$$
6. Millington formula is appropriate to estimate τ_w and τ_a :

$$\tau_w = \frac{(\theta_w)^7}{n^2} \quad \tau_a = \frac{(\theta_a)^7}{n^2} \quad (\text{Millington, 1959})$$

b. Contaminant Transport Equation:

$$\frac{\partial C_w}{\partial t} = -\left(\frac{q_{wz}}{R_w}\right) \frac{\partial C_w}{\partial z} + \frac{1}{R_w} \frac{\partial}{\partial z} \left[(D_w + D_a K_H) \frac{\partial C_w}{\partial z} \right]$$

where:

$$R_w = \theta_w + \theta_a K_H + \rho_b K_d$$

$$D_w = \left[D_{fw} + \alpha_T \left(\frac{q_{wx}}{\theta_w} \right) + \alpha_L \left(\frac{q_{wz}}{\theta_w} \right) \right] \theta_w \tau_w \quad \text{and: } D_a = D_{fa} \theta_a \tau_a$$

$$\theta_a = n - \theta_w$$

$$q_{wx} = K(\theta_w) \frac{\partial h}{\partial x} \quad \left(\frac{\partial h}{\partial x} \text{ is the hydraulic gradient} \right)$$

c. Flux Equation:

$$J = q_{wz} C_w - (D_w + D_a K_H) \frac{\partial C_w}{\partial z}$$

3. Finite-Difference Numerical Approximation of Contaminant Transport Equation
(Crank-Nicolson Method for Diffusion/Central Space Method for Advection):

a.

$$\frac{\partial C_w}{\partial t} = -\left(\frac{q_{wz}}{R_{wi}}\right) \frac{\partial C_w}{\partial z} + \frac{1}{2R_{wi}(\Delta z)^2} \left[(D_w + D_a K_H)_i (C_{wi+1}^n - C_{wi}^n + C_{wi+1}^{n+1} - C_{wi}^{n+1}) \right. \\ \left. - (D_w + D_a K_H)_{i-1} (C_{wi}^n - C_{wi-1}^n + C_{wi}^{n+1} - C_{wi-1}^{n+1}) \right]$$

c.

$$C_{wi}^{n+1} = C_{wi}^n - \frac{q_{wz} \Delta t}{4R_{wi} \Delta z} (C_{wi+1}^n - C_{wi-1}^n + C_{wi+1}^{n+1} - C_{wi-1}^{n+1}) \\ + \frac{\Delta t}{2R_{wi}(\Delta z)^2} \left[(D_w + D_a K_H)_i (C_{wi+1}^n - C_{wi}^n + C_{wi+1}^{n+1} - C_{wi}^{n+1}) \right. \\ \left. - (D_w + D_a K_H)_{i-1} (C_{wi}^n - C_{wi-1}^n + C_{wi}^{n+1} - C_{wi-1}^{n+1}) \right]$$

d. Simplify Equation:

$$\text{Let: } \lambda_{1_i} = \frac{\Delta t}{4R_{w_i}\Delta z} \quad \text{and: } \lambda_{2_i} = \frac{\Delta t}{2R_{w_i}(\Delta z)^2} \quad \text{and: } D_i = (D_w + D_a K_H)_i$$

$$\begin{aligned} \text{Thus: } C_{w_i}^{n+1} &= C_{w_i}^n - q_{wz}\lambda_{1_i} (C_{w_{i+1}}^n - C_{w_{i-1}}^n + C_{w_{i+1}}^{n+1} - C_{w_{i-1}}^{n+1}) \\ &\quad + D_i\lambda_{2_i} (C_{w_{i+1}}^n - C_{w_i}^n + C_{w_{i+1}}^{n+1} - C_{w_i}^{n+1}) \\ &\quad - D_{i-1}\lambda_{2_i} (C_{w_i}^n - C_{w_{i-1}}^n + C_{w_i}^{n+1} - C_{w_{i-1}}^{n+1}) \end{aligned}$$

e. Move All "n + 1" Terms to Left Side of Equation:

$$\begin{aligned} & - (q_{wz}\lambda_{1_i} + D_{i-1}\lambda_{2_i}) C_{w_{i-1}}^{n+1} + [1 + \lambda_{2_i} (D_i + D_{i-1})] C_{w_i}^{n+1} + (q_{wz}\lambda_{1_i} - D_i\lambda_{2_i}) C_{w_{i+1}}^{n+1} \\ & = (q_{wz}\lambda_{1_i} + D_{i-1}\lambda_{2_i}) C_{w_{i-1}}^n + [1 - \lambda_{2_i} (D_i + D_{i-1})] C_{w_i}^n - (q_{wz}\lambda_{1_i} - D_i\lambda_{2_i}) C_{w_{i+1}}^n \end{aligned}$$

f. Rewrite Solution as a Tridiagonal System of Equations:

$$\begin{array}{cccccccc|ccc|c} b_1 & e_1 & 0 & 0 & \cdot & \cdot & \cdot & 0 & 0 & C_{w_1} & & \text{RHS}_1 - a_1 C_{w_0}^{n+1} \\ a_2 & b_2 & e_2 & 0 & \cdot & \cdot & \cdot & \cdot & 0 & C_{w_2} & & \text{RHS}_2 \\ 0 & a_3 & b_3 & e_3 & \cdot & \cdot & \cdot & \cdot & \cdot & C_{w_3} & & \text{RHS}_3 \\ 0 & 0 & \cdot & \cdot & \cdot & \cdot & \cdot & \cdot & \cdot & \cdot & & \cdot \\ \cdot & \cdot & \cdot & \cdot & \cdot & \cdot & \cdot & \cdot & \cdot & \cdot & & \cdot \\ \cdot & \cdot & \cdot & \cdot & \cdot & \cdot & \cdot & 0 & 0 & \cdot & & \cdot \\ \cdot & \cdot & \cdot & \cdot & \cdot & a_{nz-3} & b_{nz-3} & e_{nz-3} & 0 & C_{w_{nz-3}} & & \text{RHS}_{nz-3} \\ 0 & \cdot & \cdot & \cdot & \cdot & 0 & a_{nz-2} & b_{nz-2} & e_{nz-2} & C_{w_{nz-2}} & & \text{RHS}_{nz-2} \\ 0 & 0 & \cdot & \cdot & \cdot & 0 & 0 & a_{nz-1} & b_{nz-1} & C_{w_{nz-1}} & & \text{RHS}_{nz-1} - e_{nz-1} C_{w_{nz}}^{n+1} \end{array} =$$

where:

$$\begin{aligned} a_i &= - (q_{wz}\lambda_{1_i} + D_{i-1}\lambda_{2_i}) & b_i &= [1 + \lambda_{2_i} (D_i + D_{i-1})] \\ e_i &= (q_{wz}\lambda_{1_i} - D_i\lambda_{2_i}) & \text{RHS}_i &= -a_i C_{w_{i-1}}^n + (2 - b_i) C_{w_i}^n - e_i C_{w_{i+1}}^n \end{aligned}$$

Note: The system is solved using the Thomas algorithm. The condition, $b_i > |a_i| + |e_i| > 0$, was used to ensure that the coefficient matrix was diagonally dominant (Mayers and Morton, 1994).

4. Finite-Difference Numerical Approximations of Flux Equation for Fluxes at Surface and at Water Table (Backward Space Method):

$$J_{\text{srf}} = q_{\text{wz}} C_{\text{w}}(z = 0) - \frac{D(z = 0)}{\Delta z} (C_{\text{w}}(z = 0) - C_{\text{w}}(z = 0 - \Delta z))$$

$$J_{\text{wt}} = q_{\text{wz}} C_{\text{w}}(z = L) - \frac{D(z = L)}{\Delta z} (C_{\text{w}}(z = L - \Delta z) - C_{\text{w}}(z = L))$$

5. Initial and Boundary Conditions:

IC: $C_{\text{w}}(z, t = 0) = 0$

BC1: $C_{\text{w}}(z = 0, t) = 0$ {at surface}

BC2: $C_{\text{w}}(z = L, t = 0..tf_1^*) = C_i$ {at water table}

$C_{\text{w}}(z = L, t = tf_1..tf_2^*) = 0$ {at water table}

* tf_1 is 2000 days

tf_2 is the time it takes for the highest aqueous concentration in the system to fall below 1 $\mu\text{g/L}$ or 2000 days

Appendix K: Analytical Solution to Simplified Contaminant Transport Equation

The following derivation was obtained from a personal communication with D. Quinn, Department of Mathematics and Statistics, Air Force Institute of Technology, OH, 18 November 1996. The method mirrors a diffusion-only approach described in Haberman (1987).

1. Simplify mass transport equation by assuming coefficients for advection, U , and diffusion-dispersion, D , are constant:

$$\text{general equation: } \frac{\partial C_w}{\partial t} = -U \frac{\partial C_w}{\partial z} + D \frac{\partial^2 C_w}{\partial z^2}$$

$$\text{with initial condition: } C_w(z, 0) = 0$$

$$\text{and boundary conditions: } C_w(0, t) = 0 \quad C_w(L, t) = C_i$$

2. Transform $C_w(z, t)$ to produce homogeneous boundary conditions:

$$\text{define: } C_w(z, t) = \frac{C_i}{L} z + V(z, t)$$

$$\text{so equation becomes: } \frac{\partial V}{\partial t} = -U \frac{C_i}{L} - U \frac{\partial V}{\partial z} + D \frac{\partial^2 V}{\partial z^2}$$

$$\text{with initial condition: } V(z, 0) = -\frac{C_i}{L} z$$

$$\text{and boundary conditions: } V(0, t) = 0 \quad V(L, t) = 0$$

3. Transform $V(z, t)$ to eliminate the $\frac{\partial V}{\partial z}$ term using a form suitable for a Fourier series:

$$\text{define: } V(z, t) = e^{\frac{Uz}{2D}} W(z, t)$$

so equation becomes:
$$\frac{\partial W}{\partial t} = -\frac{UC_i}{L} e^{-\frac{Uz}{2D}} - \frac{U^2}{4D} W + D \frac{\partial^2 W}{\partial z^2}$$

with initial condition:
$$W(z,0) = -\frac{C_i z}{L} e^{-\frac{Uz}{2D}}$$

and boundary conditions: $W(0,t) = 0 \quad W(L,t) = 0$

4. Represent $W(z,t)$ as a Fourier series which satisfies the boundary conditions $W(0,t) = 0$ and $W(L,t) = 0$:

$$W(z,t) = \sum_{n=1}^{\infty} \alpha_n(t) \sin \frac{n\pi z}{L}$$

so equation becomes:

$$\sum_{n=1}^{\infty} \alpha_n'(t) \sin \frac{n\pi z}{L} = -\frac{UC_i}{L} e^{-\frac{Uz}{2D}} - \frac{U^2}{4D} \sum_{n=1}^{\infty} \alpha_n \sin \frac{n\pi z}{L} - D \sum_{n=1}^{\infty} \alpha_n \frac{n^2 \pi^2}{L^2} \sin \frac{n\pi z}{L}$$

5. Multiply through transport equation by $\sin \frac{k\pi z}{L}$ and integrate from 0 to L:

$$\begin{aligned} \sum_{n=1}^{\infty} \alpha_n'(t) \int_0^L \sin \frac{n\pi z}{L} \sin \frac{k\pi z}{L} dz &= -\frac{UC_i}{L} \int_0^L e^{-\frac{Uz}{2D}} \sin \frac{k\pi z}{L} dz - \frac{U^2}{4D} \sum_{n=1}^{\infty} \alpha_n \int_0^L \sin \frac{n\pi z}{L} \sin \frac{k\pi z}{L} dz \\ &\quad - D \sum_{n=1}^{\infty} \alpha_n \frac{n^2 \pi^2}{L^2} \int_0^L \sin \frac{n\pi z}{L} \sin \frac{k\pi z}{L} dz \end{aligned}$$

where:
$$\int_0^L \sin \frac{n\pi z}{L} \sin \frac{k\pi z}{L} dz = \begin{cases} \frac{L}{2} & \text{if } n = k \\ 0 & \text{if } n \neq k \end{cases}$$

so equation becomes:
$$\alpha_k'(t) = -\frac{2UC_i}{L^2} \int_0^L e^{-\frac{Uz}{2D}} \sin \frac{k\pi z}{L} dz - \alpha_k \left(\frac{U^2}{4D} + D \frac{k^2 \pi^2}{L^2} \right)$$

6. Rewrite equation in the form $y'+ay = c$ and solve:

$$\text{general equation: } \alpha_k' + \omega_k \alpha_k = \gamma_k$$

$$\text{where: } \omega_k = \frac{U^2}{4D} + D \frac{k^2 \pi^2}{L^2}$$

$$\text{and: } \gamma_k = -\frac{2UC_i}{L^2} \int_0^L e^{-\frac{Uz}{2D}} \sin \frac{k\pi z}{L} dz = \frac{8k\pi D^2 UC_i}{4k^2 \pi^2 D^2 L + U^2 L^3} \left(e^{-\frac{UL}{2D}} \cos(k\pi) - 1 \right)$$

$$\text{general solution: } e^{\omega_k t} \alpha_k' + \omega_k e^{\omega_k t} \alpha_k = \gamma_k e^{\omega_k t}$$

$$\left(e^{\omega_k t} \alpha_k \right)' = \gamma_k e^{\omega_k t}$$

$$\text{integrating both sides from 0 to t: } \alpha_k(t) = \alpha_k(0) e^{-\omega_k t} + \frac{\gamma_k}{\omega_k} (1 - e^{-\omega_k t})$$

7. Apply initial condition $W(z,0) = -\frac{C_i z}{L} e^{-\frac{Uz}{2D}}$ and solve for $\alpha_k(0)$:

$$W(z,0) = \sum_{n=1}^{\infty} \alpha_n(0) \sin \frac{n\pi z}{L} = -\frac{C_i z}{L} e^{-\frac{Uz}{2D}}$$

$$\sum_{n=1}^{\infty} \alpha_n(0) \int_0^L \sin \frac{n\pi z}{L} \sin \frac{k\pi z}{L} dz = -\frac{C_i}{L} \int_0^L z e^{-\frac{Uz}{2D}} \sin \frac{k\pi z}{L} dz$$

$$\alpha_k(0) = -\frac{2C_i}{L^2} \int_0^L z e^{-\frac{Uz}{2D}} \sin \frac{k\pi z}{L} dz = \frac{2k\pi C_i}{L^2} \left[\frac{e^{-\frac{UL}{2D}} \cos(k\pi)}{\frac{U^2}{4D^2} + \frac{k^2 \pi^2}{L^2}} + \frac{U}{DL} \left(e^{-\frac{UL}{2D}} \cos(k\pi) - 1 \right) \right]$$

8. Solution:

$$C_w(z, t) = \frac{C_i}{L} z + V(z, t)$$

where:

$$V(z, t) = e^{\frac{Uz}{2D}} W(z, t)$$

$$W(z, t) = \sum_{k=1}^{\infty} \alpha_k(t) \sin \frac{k\pi z}{L}$$

$$\alpha_k(t) = \alpha_k(0) e^{-\omega_k t} + \frac{\gamma_k}{\omega_k} (1 - e^{-\omega_k t})$$

$$\alpha_k(0) = \frac{2k\pi C_i}{L^2} \left[\frac{e^{-\frac{UL}{2D}} \cos(k\pi)}{\frac{U^2}{4D^2} + \frac{k^2\pi^2}{L^2}} + \frac{\frac{U}{DL} \left(e^{-\frac{UL}{2D}} \cos(k\pi) - 1 \right)}{\left(\frac{U^2}{4D^2} + \frac{k^2\pi^2}{L^2} \right)^2} \right]$$

$$\gamma_k = \frac{8k\pi D^2 U C_i}{4k^2\pi^2 D^2 L + U^2 L^3} \left(e^{-\frac{UL}{2D}} \cos(k\pi) - 1 \right)$$

$$\omega_k = \frac{U^2}{4D} + D \frac{k^2\pi^2}{L^2}$$

Appendix L: FORTRAN computer code for Soil Water Content Model

```
*****
* PROGRAM: MODELWC - Determines Pressure Head, Conductivity, and      *
*                   Water Content as a function of Depth              *
*                   - Output file contains POR(I) and PB(I) which is  *
*                   needed in MODELCT {note: WCS=POR}                 *
*                   - PSI is defined as negative pressure head, so    *
*                   PSI(I) is positive                                *
*****
C
C
C Variable Declarations
*****
C
  IMPLICIT DOUBLE PRECISION (A-H, O-Z)
  DIMENSION PSI(0:1000), ZK(0:1000), WC(0:1000)
  CHARACTER*10 INFIL, OUTFIL, INPUT, OUTPUT
  DOUBLE PRECISION PSIA, TZK, TQZ, DQZO, DQZN, TOL, DELZ, VA, VB, VM,
  @QZ, WCS, WCR, ZKS, HB, CLAM, PB, ZL, T, Z
  COMMON QZ, WCS, WCR, ZKS, HB, CLAM, PB, ZL, T, Z
C
C
C Format Statements
*****
C
  1000 FORMAT(A10)
  2000 FORMAT('MODEL WC: Pressure head and water content vs depth',//,
  @'OUTPUT:',/,3X,'Z=Depth; PSI=Pressure Head; K=Conductivity;
  @WC=Water Content; POR=Porosity; PB=Soil Bulk Density',//,
  @7X,'Z',10X,'PSI',10X,'K',10X,'WC',9X,'POR',10X,'PB')
  3000 FORMAT(6E12.5)
  4000 FORMAT(1X//,'Solution Does Not Converge--Try Larger nz')
C
C
C Define Input/Output Files
*****
C
  WRITE(6,*) 'Name of input file'
  READ(5,1000) INFIL
  INPUT = INFIL
  WRITE(6,*) 'Name of output file'
  READ(5,1000) OUTFIL
  OUTPUT = OUTFIL
  OPEN (UNIT = 10, FILE = OUTPUT, STATUS = 'NEW')
  OPEN (UNIT = 20, FILE = INPUT, STATUS = 'OLD')
  WRITE (10, 2000)
```

```

C
C
C Calculations
*****
C
C Initialize variables
C
      TOL=0.000001
      MAXIT=1000
      NZ=0
      PSI(NZ)=0.d0
      READ(20,*) NSL,ZL,QZ
      DO 200 K=1,NSL
C
C Define Boundary Condition: Layer Above Water Table: PSI(Z=L)=0;
C                               Subsequent Layers:
C                               PSInew(Z=Z0)=PSIold(Z=Znz)
C
      PSI(0)=PSI(NZ)
      READ(20,*) WCS,WCR,ZKS,HB,CLAM,PB,T,NZ
C
C Define Parameters
C
      DELZ=T/NZ
      VA=1.d0/HB
      VB=CLAM+1.d0
      VM=CLAM/VB
      IF(K.EQ.1) Z=ZL
      IF(K.EQ.1) ZK(0)=ZKS
      IF(K.EQ.1) WC(0)=WCS
      IF(K.EQ.1) WRITE(10,3000) Z,PSI(0),ZK(0),WC(0),WCS,PB
      IF(K.EQ.1) PRINT*,Z,PSI(0),WC(0)
C
C For seed value, set PSIA=PSI(I-1) and calculate TZK
C
      DO 50 I=1,NZ
      COUNT=0
      PSIA=PSI(I-1)
      TZK=ZKS*((1.d0-(VA*PSIA)**(VB-1.d0))*(1.d0+(VA*PSIA)
      @**VB)**(-VM)**2.d0)/((1.d0+(VA*PSIA)**VB)**(VM/2.d0))
      GOTO 10

```

```

C
C Iteration Loop
C Note: Since the down direction is defined to be positive, but the
C model calculates from the water table up (-z direction):
C 1. DELZ is negative (with DELZ Z defined as Z(I)-Z(I-1))
C 2. TQZ is negative (to calculate a positive TQZ, the sign
C is changed for the right hand sign of the equation)
C
C The above comments are reflected in the equations for PSI(I)
C and TQZ below:
C
10 COUNT=COUNT+1
   IF(COUNT.GT.MAXIT) GOTO 100
   PSI(I)=(qz/TZK-1.d0)*(-DELZ)+PSI(I-1)
   IF(PSI(I).LT.0) GOTO 100
   PSIA=(PSI(I)+PSI(I-1))/2.d0
   TZK=ZKS*((1.d0-(VA*PSIA)**(VB-1.d0))*(1.d0+(VA*PSIA)
@**VB)**(-VM)**2.d0)/((1.d0+(VA*PSIA)**VB)**(VM/2.d0))
   TQZ=TZK*((PSI(I)-PSI(I-1))/(-DELZ)+1.d0)
   DQZN=QZ-TQZ
   IF(DQZN.LT.0) DQZN=-DQZN
   DQZO=DQZN
   IF(DQZO.GT.TOL) GOTO 10

C
C Calculate K and WC, and Print Results
C
   ZK(I)=TZK
   WC(I)=WCR+(WCS-WCR)/((1.d0+(VA*(PSI(I)))**VB)**VM)
   Z=Z-DELZ
   WRITE(10, 3000) Z, PSI(I), ZK(I), WC(I), WCS, PB
   PRINT*, Z, PSI(I), WC(I)
50 CONTINUE
   GOTO 200

C
100 WRITE(10, 4000)
   PRINT*, 'Solution Does Not Converge--Try Larger nz'
   GOTO 500

C
200 CONTINUE
   GOTO 500

C
500 END

```



```

C
C Iteration Loop
C Note: Since the down direction is defined to be positive, but the
C model calculates from the water table up (-z direction):
C 1. DELZ is negative (with DELZ Z defined as Z(I)-Z(I-1))
C 2. TQZ is negative (to calculate a positive TQZ, the sign
C is changed for the right hand sign of the equation)
C
C The above comments are reflected in the equations for PSI(I)
C and TQZ below:
C
10 COUNT=COUNT+1
   IF(COUNT.GT.MAXIT) GOTO 100
   PSI(I)=(qz/TZK-1.d0)*(-DELZ)+PSI(I-1)
   IF(PSI(I).LT.0) GOTO 100
   PSIA=(PSI(I)+PSI(I-1))/2.d0
   TZK=ZKS*((1.d0-(VA*PSIA)**(VB-1.d0))*(1.d0+(VA*PSIA)
@**VB)**(-VM)**2.d0)/((1.d0+(VA*PSIA)**VB)**(VM/2.d0))
   TQZ=TZK*((PSI(I)-PSI(I-1))/(-DELZ)+1.d0)
   DQZN=QZ-TQZ
   IF(DQZN.LT.0) DQZN=-DQZN
   DQZO=DQZN
   IF(DQZO.GT.TOL) GOTO 10

C
C Calculate K and WC, and Print Results
C
   ZK(I)=TZK
   WC(I)=WCR+(WCS-WCR)/((1.d0+(VA*(PSI(I)))**VB)**VM)
   Z=Z-DELZ
   WRITE(10, 3000) Z, PSI(I), ZK(I), WC(I), WCS, PB
   PRINT*, Z, PSI(I), WC(I)
50 CONTINUE
   GOTO 200

C
100 WRITE(10, 4000)
   PRINT*, 'Solution Does Not Converge--Try Larger nz'
   GOTO 500

C
200 CONTINUE
   GOTO 500

C
500 END

```

Appendix M: FORTRAN computer code for Contaminant Transport Model

```
*****
* PROGRAM: MODELCT - 1-D ADVECTIVE-DISPERSIVE TRANSPORT IN VADOSE ZONE *
* - Crank-Nicolson approximation for concentration *
* Backward space approximation for flux *
* - Z, K, WC, Pb, and porosity are read in from an *
* input file generated from WC model) *
* - Since system is stiff, allows time domain to be *
* divided up into different regions with different *
* DELT *
* - Calculates Cw, Ct, J(z=0), and J(z=L) *
*****
* Note to the reader: This code actually contains two models, one with*
* fixed boundary conditions (BCs) and one with *
* gradient BCs. For the fixed BC model, activate *
* the C1 lines, for the gradient model, activae *
* activate the C2 lines. *
*****
C
C
C Variable Declarations
*****
C
  IMPLICIT DOUBLE PRECISION (A-H, O-Z)
  DIMENSION CO(0:450), C(0:450), Z(0:450), WC(0:450), ZK(0:450),
  @POR(0:450), PB(0:450), RW(0:450), D(0:450), A(0:450), B(0:450),
  @E(0:450), RHS(0:450), G(0:450), P(0:450), R(0:450)
  CHARACTER*10 INFIL1, INFIL2, OUTFIL, INPUT1, INPUT2, OUTPUT
  DOUBLE PRECISION DELT, TO, AC, TW, TA, QWX, CLAM1, CLAM2, SA, SE, STAB,
  @CT, JSF, JWT, CI, GRAD, DFW, DFA, ZKD, ZKH, AT, AL, QWZ, Z
  COMMON CI, GRAD, DFW, DFA, ZKD, ZKH, AT, AL, QWZ
C
C
C Format Statements
*****
C
1000 FORMAT(A10)
2000 FORMAT(1X'MODEL CT: 1-D Transport Through Vadose Zone')
3000 FORMAT(1X//, 'LOADING OUTPUT:')
3100 FORMAT(1X//, 'UNLOADING OUTPUT:')
3500 FORMAT(1X/, 'Stability Requirements:',/, 1X, 'b-(|a|+|c|)>0'
  @, 1X, '|a|+|c|>0')
3600 FORMAT(2E12.5)
4000 FORMAT(1X/, 'T=Time; Z=Depth; Cw=Water Conc; Ct=Total Conc;',/,
  @'Jsf=Flux at Surface; Jwt=Flux at Water Table',/,
  @7X, 'T', 11X, 'Z', 10X, 'Cw', 10X, 'Ct', 10X, 'Jsf', 9X, 'Jwt')
5000 FORMAT(6E12.5)
```

```

C
C
C Define Input/Output Files
*****
C
  WRITE(6,*) 'Name of Parameter input file'
  READ(5,1000) INFIL1
  INPUT1 = INFIL1
  WRITE(6,*) 'Name of Water Content input file'
  READ(5,1000) INFIL2
  INPUT2 = INFIL2
  WRITE(6,*) 'Name of output file'
  READ(5,1000) OUTFIL
  OUTPUT = OUTFIL
  OPEN (UNIT = 10, FILE = OUTPUT, STATUS = 'NEW')
  OPEN (UNIT = 20, FILE = INPUT1, STATUS = 'OLD')
  OPEN (UNIT = 25, FILE = INPUT2, STATUS = 'OLD')

C
  WRITE(10,2000)
  READ(20,*) CI,GRAD,DFW,DFA,ZKD,ZKH
  READ(20,*) NZ,NTR,NTL,AT,AL,QWZ
  DO 10 I=0,NZ
    READ (25,*) Z(I),ZK(I),WC(I),POR(I),PB(I)
10  CONTINUE
C
C Define Parameters
C
  DO 20 I=0,NZ
    AC=POR(I)-WC(I)
    TW=(WC(I)**(7.d0/3.d0))/(POR(I)**2.d0)
    TA=(AC**(7.d0/3.d0))/(POR(I)**2.d0)
    QWX=ZK(I)*GRAD
    D(I)=(DFW+AT*QWX/WC(I)+AL*QWZ/WC(I))*WC(I)*TW+DFA*AC*TA*ZKH
    RW(I)=WC(I)+AC*ZKH+PB(I)*ZKD
20  CONTINUE
C
C Begin Time Region Loop
C
  TO=0
  DO 900 U=1,NTR
    IF(U.LE.NTL) WRITE(10,3000)
    IF(U.GT.NTL) WRITE(10,3100)
    WRITE(10,3500)
    READ (20,*) TF,NT
    DELT=TF/NT

```

```

C
C Define Parameters which are Dependent on DELT
C
DO 50 I=1,NZ-1
  CLAM1=DELT/(4.d0*RW(I)*(Z(I)-Z(I-1)))
  CLAM2=DELT/(2.d0*RW(I)*((Z(I)-Z(I-1))**2.d0))
  A(I)=-(QWZ*CLAM1+D(I-1)*CLAM2)
  B(I)=1.d0+CLAM2*(D(I)+D(I-1))
  E(I)=QWZ*CLAM1-D(I)*CLAM2
  IF(A(I).LT.0) SA=-A(I)
  IF(A(I).GE.0) SA=A(I)
  IF(E(I).LT.0) SE=-E(I)
  IF(E(I).GE.0) SE=E(I)
  STAB=B(I)-(SA+SE)
  WRITE(10,3600) STAB, SA+SE
50  CONTINUE
  WRITE(10,4000)
  IF(U.EQ.1) GOTO 100
  IF(U.EQ.NTL+1) GOTO 200
  GOTO 500
C
C
C Define Initial Condition
*****
C
C LOADING Phase: C(Z,T=0)=0
C Note: Since CO is zero, no unit conversion is necessary
C
100  T=0.d0
    CT=0.d0
    JSF=0.d0
    JWT=0.d0
    DO 120 I=0,NZ
      CO(I)=0.d0
      WRITE(10, 5000) T, Z(I), CO(I), CT, JSF, JWT
      PRINT*, T, Z(I), CO(I)
120  CONTINUE
    GOTO 300

```

```

C
C UNLOADING Phase: C(Z,T=TF1)
C {final result from LOADING Phase except C(Z=L,T=TF1)=0}
C Note: Convert CO back to ppm and J to g/m^2 for printing
C
C1 200 CO(0)=0.d0
C1 DO 220 I=0,NZ
C2 200 DO 220 I=0,NZ
      CT=CO(I)*RW(I)
      JWT=QWZ*CO(0)-D(0)/(Z(1)-Z(0))*(CO(1)-CO(0))
      WRITE(10, 5000) T, Z(I), CO(I)*1000000.d0, CT*1000000.d0,
      @JSF*10000.d0, JWT*10000.d0
      PRINT*, T, Z(I), CO(I)*1000000.d0
220 CONTINUE
      GOTO 400
C
C
C Boundary Conditions
*****
C
C LOADING Phase: C(Z=0,T=0..TF1)=0; C(Z=L,T=0..TF1)=CI
C Note: C must first be converted from ppm (g/m^3) to g/cm^3)
C
C1 300 CO(0)=CI/1000000.d0
C1 CO(NZ)=0.d0
C2 300 CO(NZ)=0.d0
C1 C(0)=CI/1000000.d0
      C(NZ)=0.d0
      GOTO 500
C
C UNLOADING Phase: C(Z=0,T=TF1..TF2)=0; C(Z=L,T=TF1..TF2)=0
C
400 CO(NZ)=0.d0
C1 C(0)=0.d0
      C(NZ)=0.d0
      GOTO 500

```

```

C
C
C Solve using Thomas algorithm
*****
C
500     G(1)=E(1)/B(1)
      DO 520 J=2,NZ-1
          P(J)=B(J)-A(J)*G(J-1)
          G(J)=E(J)/P(J)
520     CONTINUE
      DO 600 N=1,NT
C2     IF (U.LE.NTL.AND.T+DELT.LE.200) C(0)=(T+DELT)*(CI
C2     @/1000000.d0)/200.d0
C2     IF (U.LE.NTL.AND.T+DELT.GT.200) C(0)=CI/1000000.d0
C2     IF (U.GT.NTL.AND.T+DELT.LE.2200) C(0)=CI/1000000.d0
C2     @*(1-(T-2000+DELT)/200.d0)
C2     IF (U.GT.NTL.AND.T+DELT.GT.2200) C(0)=0.d0
      RHS(1)=-A(1)*CO(0)+(2-B(1))*CO(1)-E(1)*CO(2)-A(1)*C(0)
      R(1)=RHS(1)/B(1)
      DO 540 J=2,NZ-2
          RHS(J)=-A(J)*CO(J-1)+(2-B(J))*CO(J)-E(J)*CO(J+1)
          R(J)=(RHS(J)-A(J)*R(J-1))/P(J)
540     CONTINUE
      RHS(NZ-1)=-A(NZ-1)*CO(NZ-2)+(2-B(NZ-1))*CO(NZ-1)-E(NZ-1)
      @*CO(NZ)-E(NZ-1)*C(NZ)
      C(NZ-1)=(RHS(NZ-1)-A(NZ-1)*R(NZ-2))/P(NZ-1)
      DO 560 K=1,NZ-2
          C(NZ-1-K)=R(NZ-1-K)-G(NZ-1-K)*C(NZ-K)
560     CONTINUE
      DO 580 I=0,NZ
          T=N*DELT+TO
          CT=C(I)*RW(I)
          JSF=QWZ*C(NZ)-D(NZ)/(Z(NZ)-Z(NZ-1))*(C(NZ)-C(NZ-1))
          JWT=QWZ*C(0)-D(0)/(Z(1)-Z(0))*(C(1)-C(0))
C
C Convert C back to ppm and J to g/m^2 for printing
C
      WRITE(10,5000) T,Z(I),C(I)*1000000.d0,CT*1000000.d0,
      @JSF*10000.d0,JWT*10000.d0
      PRINT*,T,Z(I),C(I)*1000000.d0
      CO(I)=C(I)
580     CONTINUE
600     CONTINUE
      TO=T
900     CONTINUE
C
      END

```

References

- Abriola, L. M. (1989). "Modeling Multiphase Migration of Organic Chemicals in Groundwater Systems -- A Review and Assessment," *Environmental Health Perspectives*, 83: 117-143.
- Abriola, L. M. and Pinder, G. F. (1986). "On the Simulation of Nonaqueous Phase Organic Compounds in the Subsurface," *Water Resources Research*, 22(9): 109S-119S.
- Alzaydi, A. A., Moore, C. A., and Rai, I. S. (1978) "Combined Pressure and Diffusional Transition Region Flow of Gases in Porous Media," *AIChE Journal*, 24(1): 35-42.
- Baehr, A. L. (1987). "Selective Transport of Hydrocarbons in the Unsaturated Zone Due to Aqueous and Vapor Phase Partitioning," *Water Resources Research*, 23(10): 1926-1938.
- Barber, C., Briegel, D., Davis, G. B., and Ward J. K. (1990) "Factors Controlling the Concentration of Methane and Other Volatiles in Ground-water and Soil-gas Around a Waste Site," *Journal of Contaminant Hydrology*, 5: 155-169.
- Buckingham, E. (1907) "Studies on the Movement of Soil Moisture," *U. S. Department of Agriculture Bureau of Soils Bulletin*, 38.
- Chiou, C. T., Freed, V. H., and Peters, L. J. (1979). "A Physical Concept of Soil-Water Equilibria for Nonionic Organic Compounds," *Science*, 206: 831-832.
- Chiou, C. T. and Shoup, T. D. (1985). "Soil Sorption of Organic Vapors and Effects of Humidity on Sorptive Mechanism and Capacity," *Environmental Science and Technology*, 19: 1196-1200.
- Conant, B. H., Gillham, R. W., and Mendoza, C. A. (1996) "Vapor Transport of Trichloroethylene in the Unsaturated Zone," *Water Resources Research*, 32(1): 9-22.
- Culver, T. B., Lion, L. W., and Shoemaker, C. A. (1991). "Impact of Vapor Sorption on the Subsurface Transport of Volatile Organic Compounds: A Numerical Model and Analysis," *Water Resources Research*, 27(9): 2259-2270.

- Culver, T. B., Lion, L. W., Ong, S. K., and Shoemaker, C. A. (1992). "Effects of Soil Moisture and Physical-chemical Properties of Organic Pollutants in Vapor-phase Transport in the Vadose Zone," *Journal of Contaminant Hydrology*, 11: 273-290.
- Department of the Air Force. (1994). *McClellan Air Force Base Final Interim Basewide Remedial Investigation -- Part 1: General Framework*. USAF Contract No. F33615-90-D-4013.
- Dragun, J., Kuffner, A. C., and Schneiter, R. W. (1984). "Groundwater Contamination - Part I: Transport and Transformation of Organic Chemicals," *Chemical Engineering*, 91(24): 65-70.
- Dyksen, J. E., and Hess, A. F. (1982). "Alternatives for Controlling Organics in Groundwater supplies," *Journal of the American Water Works Association*, 74: 394.
- Earp, D. E., Thompson, G. L., and Weeks, E. P. (1982). "Use of Atmospheric Fluorocarbons F-11 and F-12 to Determine the Diffusion Parameters of the Unsaturated Zone in the Southern High Plains of Texas," *Water Resources Research*, 18(5): 1365-1378.
- Falta, R. W., Javandel, I., Pruess, K., and Witherspoon, P. A. (1989). "Density-driven Flow of Gas in the Unsaturated Zone Due to the Evaporation of Volatile Organic Compounds," *Water Resources Research*, 25(10): 2159-2169.
- Farmer, W. J., Letey, J., Spencer, W. F., and Yang, M. S. (1980). "Hexachlorobenzene: Its Vapor Pressure and Vapor Phase Diffusion in Soil," *Soil Science Society of America Journal*, 44: 676-680.
- Farrier, D. F., and Massmann, J. (1992). "Effects of Atmospheric Pressures on Gas Transport in the Vadose Zone," *Water Resources Research*, 28(3): 777-791.
- Faust, C. R. (1985) "Transport of Immiscible Fluids Within and Below the Unsaturated Zone: A Numerical Model," *Water Resources Research*, 21(4): 587-596.
- Fetter, C. W. (1993). *Contaminant Hydrology*. Upper Saddle River NJ: Prentice-Hall, Inc.
- Frind, E. O. and Mendoza, C. A. (1990a). "Advection-dispersive Transport of Dense Organic Vapors in the Unsaturated Zone: 1. Model Development," *Water Resources Research*, 26(3): 379-387.

- Frind, E. O. and Mendoza, C. A. (1990b). "Advection-dispersive Transport of Dense Organic Vapors in the Unsaturated Zone: 2. Sensitivity Analysis," *Water Resources Research*, 26(3): 388-398.
- Haberman, R. (1987). *Elementary Applied Partial Differential Equations with Fourier Series and Boundary Value Problems*. 2nd ed. Englewood Cliffs NJ: Prentice-Hall, Inc.
- Howe, G. B., Mullins, M. E., and Rogers, T. N. (1986). *Evaluation and Prediction of Henry's Law Constants and Aqueous Solubilities for Solvents and Hydrocarbon Fuel Components -- Vol I: Technical Discussion*. Final Report to the Air Force Engineering and Services Center.
- Johnson, R. L. and McCarthy, K. A. (1993). "Transport of Volatile Organic Compounds Across the Capillary Fringe," *Water Resources Research*, 29(6): 1675-1683.
- Kerfoot H. B., and Marrin, D. L. (1988). "Soil-gas Surveying Techniques," *Environmental Science and Technology*, 22(7): 740-745.
- Kreamer, D. K., Thompson, G. M., and Weeks, E. P. (1988) "A Field Technique to Measure the Tortuosity and Sorption-affected Porosity for Gaseous Diffusion of Materials in the Unsaturated Zone with Experimental Results from Near Barnwell, South Carolina," *Water Resources Research*, 24(3): 331-341.
- Lion, L. W., Peterson, M. S., and Shoemaker, C. A. (1988). "Influence of Vapor-phase Sorption and Diffusion on the Fate of Trichloroethylene in an Unsaturated Aquifer System," *Environmental Science Technology*, 22(5): 571-578.
- Lyman, W. J., Reehl, W. F., and Rosenblatt, D. H. (1982). *Handbook of Chemical Property Estimation Methods: Environmental Behavior of Organic Chemicals*. New York: McGraw-Hill Book Co.
- Maidment, D. R. (1983). *Handbook of Hydrology*. New York: McGraw-Hill, Inc.
- Marrin, Donn L., and Thompson, G. M. (1987). "Gaseous Behavior of TCE Overlying a Contaminated Aquifer," *Ground Water*, 25(1): 21-27.
- Mayers, D. F. and Morton, K. W. (1994). *Numerical Solution of Partial Differential Equations*. Melbourne Australia: Cambridge UP.
- McAlary, T. A. and Mendoza, C. A. (1990). "Modeling of Ground-water Contamination by Organic Solvent Vapors," *Ground Water*, 28(2): 199-206.

- Merz, P. H. and Mohr, D. H. (1995). "Application of a 2D Air Flow Model to Soil Vapor Extraction and Bioventing Case Studies," *Ground Water*, 33(3): 433-444.
- Millington, R. J. (1959) "Gas Diffusion in Porous Media," *Science*, 130: 100-102.
- Sleep, B., and Sykes, J. F. (1989). "Modeling the Transport of Volatile Organics in Variably Saturated Porous Media," *Water Resources Research*, 25(1): 81-92.
- Tietenberg, T. (1994). *Environmental Economics and Policy*. New York: HarperCollins College Publishers.
- van Genuchten, M. Th. (1980). "A Closed-form Equation for Predicting the Hydraulic Conductivity of Unsaturated Soils," *Soil Science Society of America Journal*, 44: 892-898.

Vita

Capt Monte S. Harner was born on 22 October 1968 [REDACTED]

He graduated from Line Mountain High School in 1988 and entered the United States Air Force Academy in Colorado Springs, Colorado. On 27 May 1992, he graduated with a Bachelor of Science degree in Civil Engineering and received a regular commission into the United States Air Force. He married Leigh E. Nye of Sunbury, Pennsylvania, on [REDACTED]

[REDACTED]

Capt Harner's first assignment was to the 438th (and later 305th) Civil Engineer Squadron at McGuire AFB, New Jersey. While there, he held positions as project manager; readiness flight chief; and engineering flight assistant chief. During this time, he was also deployed to Riyadh, AFB, Saudi Arabia, as operations element chief for the 4409th (P) Civil Engineer Flight, in support of Operation Southern Watch. In May 1995, he entered the School of Engineering, Air Force Institute of Technology at Wright-Patterson AFB, Ohio. After graduating in December, 1996, with a Master of Science degree in Engineering and Environmental Management, he reported to Howard, AFB, Panama.

[REDACTED]

REPORT DOCUMENTATION PAGE

Form Approved
OMB No. 0704-0188

Public reporting burden for this collection of information is estimated to average 1 hour per response, including the time for reviewing instructions, searching existing data sources, gathering and maintaining the data needed, and completing and reviewing the collection of information. Send comments regarding this burden estimate or any other aspect of this collection of information, including suggestions for reducing this burden, to Washington Headquarters Services, Directorate for Information Operations and Reports, 1215 Jefferson Davis Highway, Suite 1204, Arlington, VA 22202-4302, and to the Office of Management and Budget, Paperwork Reduction Project (0704-0188), Washington, DC 20503.

1. AGENCY USE ONLY (Leave blank)		2. REPORT DATE December 1996	3. REPORT TYPE AND DATES COVERED Master's Thesis	
4. TITLE AND SUBTITLE MASS TRANSPORT OF VOLATILE ORGANIC COMPOUNDS BETWEEN THE SATURATED AND VADOSE ZONES			5. FUNDING NUMBERS	
6. AUTHOR(S) MONTE S. HARNER, CAPT, USAF				
7. PERFORMING ORGANIZATION NAME(S) AND ADDRESS(ES) Air Force Institute of Technology (AFIT) Wright Patterson AFB, OH 45433-7765			8. PERFORMING ORGANIZATION REPORT NUMBER AFIT/GEE/ENV/96D-05	
9. SPONSORING / MONITORING AGENCY NAME(S) AND ADDRESS(ES) HQ AFMC/CEVR Wright Patterson AFB, OH 45433-5754			10. SPONSORING / MONITORING AGENCY REPORT NUMBER	
11. SUPPLEMENTARY NOTES				
12a. DISTRIBUTION / AVAILABILITY STATEMENT Approved for public release; distribution unlimited			12b. DISTRIBUTION CODE	
13. ABSTRACT (Maximum 200 words) Volatile organic compounds (VOCs) dissolved in the saturated zone are transported into the vadose zone primarily by gaseous phase diffusion. If the saturated zone is remediated, VOCs present in the vadose zone may become a secondary source of contamination for the groundwater. The amount of VOCs that remain in the vadose zone is dependent on site hydrology, soil properties, and the chemical properties of the contaminants. The purpose of this study was to determine what conditions caused VOC concentrations in the vadose zone to significantly recontaminate the saturated zone. A one-dimensional numerical model was developed to investigate the transport of a VOC, trichloroethylene, between the saturated and vadose zones under a variety of conditions. The model featured steady-state unsaturated water flow and transient contaminant transport. Transport mechanisms included aqueous phase advection-dispersion and gaseous phase diffusion. Partitioning between the water, gas, and soil compartments were modeled as equilibrium processes. Sensitivity analyses were performed on several variables including soil type (homogeneous and heterogeneous profiles), water infiltration rate, and vadose zone depth. Results indicated that recontamination was most significant in the presence of heterogeneous soils, low infiltration rates and deep vadose zones.				
14. SUBJECT TERMS contaminant transport, finite difference, infiltration, numerical modeling, unsaturated transport, unsaturated zone, water infiltration, water flow, vadose zone, voc, volatile organic compound			15. NUMBER OF PAGES 96	
17. SECURITY CLASSIFICATION OF REPORT Unclassified			16. PRICE CODE	
18. SECURITY CLASSIFICATION OF THIS PAGE Unclassified		19. SECURITY CLASSIFICATION OF ABSTRACT Unclassified		20. LIMITATION OF ABSTRACT UL